Supporting Information

Ionic Liquid Droplet Micro-Reactor for Catalysis Reactions not at Equilibrium

Ming Zhang, Rammile Ettelaie, Tao Yan, Suojiang Zhang, Fangqin Cheng, Bernard P. Binks and Hengquan Yang*

Experimental Section

Mass Spectrometry Spectra

1. Chemicals

Dimethyldichlorosilane, (*R, S*)-1-phenylethyl alcohol (98%), (*R, S*)-1-phenylethylamine (98%), (*R, S*)-1-phenyl-1-propanol (97%), vinyl acetate (99%), n-hexylamine, rhodamine B (99%), CuI (99%), phenylacetylene (97%), 1-hexyne (97%) and fluorescein isothiocyanate isomer I (FITC-I, CAS No.3326-32-7) were purchased from Aladdin (China). (*R, S*)-4-phenyl-2-butanol (98%), ethyl methoxyacetate, trimethylsilyl cyanide and benzyl azide were purchased from Adamas Reagent Co., Ltd, (China). (*R, S*)-1-Indanol (98%) and (*R, S*)-4-methyl-2-pentanol (99%) were purchased from Alfa Aesar. (*R, S*)-5-Methyl-3-hexanol (99%) and Nile red (CAS No. 7385-67-3) were obtained from Sigma-Aldrich. Native Lipase B from *Candida Antarctica* (CALB) was purchased from Novozymes. 1-Butyl-3-methylimidazolium hexafluorophosphate (99%), 1-butyl-3-methylimidazolium tetrafluoroborate (99%), 1-butyl-3-methylimidazolium nitrate (99%) and 1-butyl-3-methylimidazolium bis(trifluoromethylsulfonyl)imide (99%) were purchased from Lanzhou Institute of Chemical Physics, Chinese Academy of Sciences. Water used in this study was de-ionized water.

2. Characterization

Nitrogen-sorption analysis of silica emulsifier was performed at -196 ℃ on a Micromeritics ASAP 2020 analyzer. Before measurement, samples were out gassed at 120 °C under vacuum for 6 h. The specific surface area was calculated from the adsorption branch in the relative pressure range of 0.05–0.15 using the Brunauer-Emmett-Teller (BET) method. Samples for transmission electron microscopy (TEM) observation were prepared by dispersing the sample powder in ethanol using ultrasound and then allowing a drop of the suspension to evaporate on a copper gird covered with a holey carbon film. TEM images were obtained on a JEOL-JEM-2000EX instrument. Emulsion droplets were observed using an optical microscope analyzer (XSP-8CA, Shanghai, China) equipped with 4 or 10 × magnification lens. X-ray photoelectron spectra (XPS) ware recorded on a Kratos Axis Ultra DLD. The contact angles of water in air on silica particle disks were measured using a Krüss DSA100 instrument. Before measurement, the powder sample was compressed into a disk of thickness approximately 1 mm (*ca*. 2 MPa). A drop of water (1 μL) was formed on the sample disk. The appearance of the water droplet was recorded at *ca*. 0.1 s with a digital camera. The value of the contact angle was determined by a photogoniometric method. Gas chromatography (GC) analysis was carried out on an Agilent 7890 analyzer (Agilent HP-5 or Agilent-19091G-B213, HP-CHIRAL-20B) with a flame ionization detector. The identification of products by mass spectrometry (MS) was performed on a GC-MS instrument (7890A-5977A, HP-5, Agilent). Confocal laser scanning microscopy images were obtained on a Carl Zeiss LSM880 instrument (Germany). The concentration of FITC-I in ionic liquid was 2×10^{-6} M and the excitation wavelength is 488 nm (green). The concentration of Nile Red in *n*-octane was 5×10^{-6} M and the excitation wavelength is 559 nm (red). The concentration of Rhodamine B in water was 2×10^{-3} M and the excitation wavelength is 554 nm (red).

3. Material Synthesis

Preparation of silica emulsifier. Silica nanoparticles were prepared *via* a modified Stöber method.[1] 1.0 g as-synthesized silica nanospheres (dried at 120 °C for 4 h) were dispersed into 12 mL toluene using sonication for 20 min. 3 mmol $(CH_3)_2SiCl_2$ and 6 mmol $CH_3(CH_2)_5NH_2$ (as catalyst) was then added into this suspension. This mixture was stirred under a N_2 atmosphere at 60 °C. After 4 h, the solid particles were collected through centrifugation. After washing with toluene and methanol, dimethyl-modified silica particles were obtained as emulsifier.

Preparation of rhodamine B-labeled enzyme. 2 mL native CALB and 200 μL Rhodamine B solution (2×10^{-3} M) were added to a 2 mL PBS solution (phosphate buffer: 0.05 M Na_2HPO_4–0.05 M NaH_2PO_4,

pH 8.0). This solution was stirred for 12 h at room temperature in the dark. After removal of the residual Rhodamine B through centrifugation, the solid was isolated then washed with PBS four times leading to the Rhodamine B-labeled CALB.

Preparation of FITC-I-labelled emulsifier. 1.0 g of dimethyl-modified silica particles and 0.001 mmol $(CH_3CH_2O)_3SiCH_2CH_2CH_2NH_2$ were dispersed into 8 ml toluene. This mixture was stirred under a N_2 atmosphere at 60 °C. After 2 h, the solid particles were collected through centrifugation, washed four times with toluene and dried, resulting in bifunctionalized silica nanospheres. 0.5 g of this bifunctionalized silica particles and 0.005 g fluorescein isothiocyanate isomer I (FITC-I) were dispersed into 50 ml ethanol. The mixture was stirred overnight at room temperature in the dark. After centrifugation, the solid was washed five times with ethanol and dried yielding FITC-I-labelled emulsifier.

4. General Procedure for Preparing IL-in-Oil Pickering Emulsions.

A given volume of oil phase containing solid emulsifier was added to a given quality of ionic liquid ([BMIM]PF_6 or [BMIM]NTf_2 or [BMIM]BF_4 or [BMIM]NO_3). Vigorous shearing (8000 rpm for 2 min) the mixture by a homogenizer generated an IL-in-oil Pickering emulsion.

5. Permeability of IL Droplet to Probe Molecules

IL-in-oil Pickering emulsion droplets were deposited on a glass slide and diluted with *n*-octane. 5 μL of Nile Red solution (5 μM in *n*-octane) was gently dropped on the glass slide. The diffusion of Nile Red molecules into the droplets was recorded by fluorescence microscopy at intervals. Similarly, ionic liquid containing FITC-I (2 μM) was used to prepare IL-in-oil Pickering emulsions. The FITC-I-containing droplets were deposited on a glass slide and 5 μL of a mixture of ethanol in *n*-octane (30% v/v) was gently dropped on the glass slide. The diffusion of Nile Red from the IL droplets to the continuous oil phase was recorded by fluorescence microscopy at intervals.

6. Determination of Partition Coefficient of Organic Compound between IL and Oil

A mixture of 1 mL of oil containing a given organic compound (0.1 M) and 1 mL of ionic liquid was stirred for 12 h at room temperature to reach equilibrium. After phase separation, the concentration of the compound in the oil phase was determined by GC. The concentration of this compound in the ionic liquid is calculated from the difference between the initial concentration in oil and the determined concentration after equilibrium. This experiment was repeated three times to obtain an average value. The partition coefficient ($K_{IL/oil}$) between ionic liquid and oil is the ratio of the compound concentration in the ionic liquid to that in the oil at equilibrium.

Partition coefficient of organic compounds between [BMIM]PF_6 and a mixture of *n*-octane and toluene (v/v = 1:1) .

Organic compound (0.1 M)	Benzyl azide	Phenyl acetylene	1-Benzyl-4-phenyl-1,2,3-triazole
$K_{IL/oil}$	2.5	1.5	2

7. IL droplet-based continuous flow reactions

CALB-catalyzed enantioselective trans-esterification of alcohols and amidation of amine. A mixture of 6.5 g [BMIM]PF_6 containing 80 μL (for alcohols) or 240 μL (for amine) aqueous enzyme solution (4 mg mL^{-1} of protein; pH 8.0), 2.4 mL *n*-octane or toluene and 0.195 g emulsifier was stirred at 8000 rpm for 1 min yielding an IL-in-oil Pickering emulsion. This Pickering emulsion was gently

poured into a glass column reactor (inner diameter is 2 cm), whose bottom is a sand filter (4.5–9 μm in pore diameter). A solution of racemic alcohol (0.1 M) or racemic amine (0.05 M) and vinyl acetate (for alcohols, 0.4 M) or ethyl methoxyacetate (for amine, 0.2 M) in *n*-octane or toluene as mobile phase was pumped through the inlet of the column reactor at a given flow rate and was allowed to pass through the column reactor whose temperature was kept at 45 °C. The outflow from the outlet of the column reactor was sampled for GC at intervals. The product was further confirmed with GC-MS.

CuI-catalyzed azide–alkyne cycloadditions. A mixture of 2 g [BMIM]PF_6, 0.032 g CuI, 0.16 g L-ascorbic acid sodium (as antioxidant), 0.7 mL of a mixture of *n*-octane and toluene (v/v = 1:1) and 0.06 g emulsifier was stirred at 8000 rpm for 1 min yielding an IL-in-oil Pickering emulsion. This Pickering emulsion was gently poured into a glass column reactor (inner diameter is 2 cm), whose bottom is a sand filter (4.5–9 μm in pore diameter). A solution of benzyl azide (0.1 M) and alkyne (0.12 M) in a mixture of *n*-octane and toluene (v/v = 1:1) as mobile phase was pumped through the inlet of the column reactor at a given flow rate and was allowed to pass through the column reactor whose temperature was kept at 25 °C. The outflow from the outlet of the column was collected for GC at intervals. The product was further confirmed with GC-MS.

8. Batch Reactions

CALB-catalyzed enantioselective trans-esterification of alcohols and amidation of amine. The batch biphasic reactions were conducted in a 10 mL glass vial. 2 g [BMIM]PF_6 containing 25 μL (for alcohols) or 75 μL (for amine) aqueous enzyme solution (4 mg mL^{-1} of protein; pH 8.0), 1 mL *n*-octane or toluene containing racemic alcohols (0.1 M) or racemic amine (0.05 M) and vinyl acetate (for alcohols, 0.4 M) or ethyl methoxyacetate (for amine, 0.2 M) were charged into this vial. The reaction mixture was stirred with a magnetic bar (10 mm in length, 2600 rpm) at 45 °C. Aliquots of the solution were taken at intervals and extracted with diethyl ether for monitoring conversions by chiral GC.

CuI-catalyzed azide–alkyne cycloadditions. The batch biphasic reactions were conducted in a 10 mL glass vial. 2 g [BMIM]PF_6, 0.032 g CuI, 0.16 g L-ascorbic acid sodium (as antioxidant), 1 mL of a mixture of *n*-octane and toluene (v/v = 1:1) containing benzyl azide (0.1 M) and (0.12 M) alkyne were charged into this vial. The reaction mixture was stirred a magnetic bar (10 mm in length, 2600 rpm) at 25 °C. Aliquots of the solution were taken and extracted with diethyl ether at intervals for monitoring conversions by GC.

9. Detailed Derivation Process of Equations for Theoretical Investigation.

Definitions

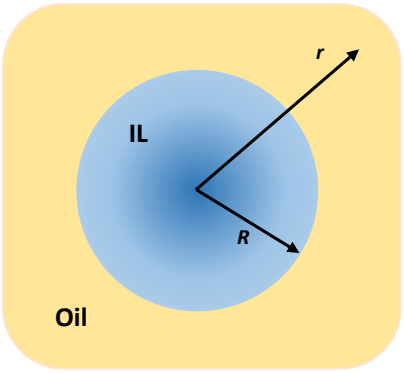

R – Radius of IL droplet

r – Distance from centre of droplet

K – Equilibrium constant of reaction

k_1 – Rate constant of forward reaction in IL

k_2 – Rate constant of backward reaction in IL

$[A]$ – Concentration of reactant A

$[B]$ – Concentration of reactant B

$[C]$ – Concentration of product C

D_{IL}^{A} – Diffusion coefficient of A in IL

D_{IL}^{B} – Diffusion coefficient of B in IL

D_{IL}^{C} – Diffusion coefficient of C in IL

D_{Oil}^{A} – Diffusion coefficient of A in oil

D_{Oil}^{B} – Diffusion coefficient of B in oil

D_{Oil}^{C} – Diffusion coefficient of C in oil

Derivation

To theoretically describe the localized reactions occurring inside a single droplet, a model reaction of A+B $\rightleftharpoons$ C is considered here. Under steady state conditions, we obtain the following equations according to the mass balance:

$$\frac{D_{IL}^{A}}{r^2}\frac{\partial}{\partial r}\left(r^2\frac{\partial[A]}{\partial r}\right)-k_1[A][B]+k_2[C]=0 \quad (1)$$

$$\frac{D_{IL}^{B}}{r^2}\frac{\partial}{\partial r}\left(r^2\frac{\partial[B]}{\partial r}\right)-k_1[A][B]+k_2[C]=0 \quad (2)$$

$$\frac{D_{IL}^{C}}{r^2}\frac{\partial}{\partial r}\left(r^2\frac{\partial[C]}{\partial r}\right)+k_1[A][B]-k_2[C]=0 \quad (3)$$

Adding equation (1) and (3) together, we obtain

$$\frac{1}{r^2}\frac{\partial}{\partial r}\left(r^2\frac{\partial\left(D_{IL}^{C}[C]+D_{IL}^{A}[A]\right)}{\partial r}\right)=0 \quad (4)$$

Integrating the equation twice, we have

$$D_{IL}^{C}[C]+D_{IL}^{A}[A]=-\frac{Q}{r}+q \quad (5)$$

where *Q* and *q* are constants of integration to be determined by the boundary conditions. We note that the value of $D_{IL}^{C}[C]+D_{IL}^{A}[A]$ has to remain finite everywhere inside the droplet and therefore Q = 0. We arrive at the following relation between the concentrations of A and C inside the droplet

$$[A]=\frac{q-D_{IL}^{C}[C]}{D_{II}^{A}} \quad (6)$$

Substitute the above equation in (3) and consider the resulting equation under the condition that the concentration of B is very large and far in excess of A. In such a case it is reasonable to take the concentration of B in the droplet as uniform everywhere. We denote this constant concentration of B as $[B]_{IL}^{0}$. In such a system we therefore have

$$\frac{1}{r^2}\frac{\partial}{\partial r}\left(r^2\frac{\partial[C]}{\partial r}\right)=-\frac{k_1[B]_{IL}^{0}}{D_{IL}^{C}}\left[\frac{q-D_{IL}^{C}[C]}{D_{IL}^{A}}\right]+\frac{k_2[C]}{D_{IL}^{C}} \quad (7)$$

where we take $[B]_{IL}^{0}=\alpha_B[B]_{Oil}^{0}$, as given by the partitioning of B between IL and oil. We now define the following constants

$$\lambda=\frac{k_1[B]_{IL}^{0}q}{D_{IL}^{C}D_{IL}^{A}} \quad (8)$$

$$\zeta^{-2}=\frac{k_1[B]_{IL}^{0}}{D_{IL}^{A}}+\frac{k_2}{D_{IL}^{C}} \quad (9)$$

Then equation (7) can be simplified as follows

$$\frac{1}{r^2}\frac{\partial}{\partial r}\left(r^2\frac{\partial[C]}{\partial r}\right)=-\lambda+\zeta^{-2}[C] \quad (10)$$

The above equation can be solved by defining $y = r[C]$, and substituting this in (10) to yield:

$$\frac{\partial^2 y}{\partial r^2}-\zeta^{-2}y=-\lambda r \quad (11)$$

The solution to the above equation is

$$y=\lambda\zeta^2 r+me^{-r/\zeta}+ne^{+r/\zeta} \quad (12)$$

where *m* and *n* are integration constants to be determined by the boundary condition. This then gives

$$[\mathrm{C}] = \lambda\zeta^2 + \frac{\mathrm{m}e^{-\mathrm{r}/\zeta}}{\mathrm{r}} + \frac{\mathrm{n}e^{+\mathrm{r}/\zeta}}{\mathrm{r}} \tag{13}$$

Now the value of *C* has to remain finite as $r \to 0$. This then means that $m = -n$, *i.e.*

$$\mathrm{C}(\mathrm{r}) = \lambda\zeta^2 + \frac{2\mathrm{n}}{\mathrm{r}}\sinh(\mathrm{r}/\zeta) \tag{14}$$

The concentration of A is then consequently given by substituting (14) into (6):

$$\mathrm{A}(\mathrm{r}) = \frac{\mathrm{q}}{\mathrm{D}_{\mathrm{IL}}^{\mathrm{A}}} - \frac{\mathrm{D}_{\mathrm{IL}}^{\mathrm{C}}}{\mathrm{D}_{\mathrm{IL}}^{\mathrm{A}}}\left(\lambda\zeta^2 + \frac{2\mathrm{n}}{\mathrm{r}}\sinh(\mathrm{r}/\zeta)\right) = \frac{\mathrm{q}}{\mathrm{D}_{\mathrm{IL}}^{\mathrm{A}}}\left(1 - \frac{\mathrm{K}[\mathrm{B}]_{\mathrm{IL}}^0\,\mathrm{D}_{\mathrm{IL}}^{\mathrm{C}}}{\mathrm{K}[\mathrm{B}]_{\mathrm{IL}}^0\,\mathrm{D}_{\mathrm{IL}}^{\mathrm{C}} + \mathrm{D}_{\mathrm{IL}}^{\mathrm{A}}}\right) - \frac{2\mathrm{n}\mathrm{D}_{\mathrm{IL}}^{\mathrm{C}}\sinh(\mathrm{r}/\zeta)}{\mathrm{r}\mathrm{D}_{\mathrm{IL}}^{\mathrm{A}}} \tag{15}$$

In the oil phase, the reaction kinetics is extremely slow and therefore to a first approximation can be neglected. In oil phase then the reaction-diffusion equations simply become the diffusion equations. For A and C these read

$$\frac{\mathrm{D}_{\mathrm{Oil}}^{\mathrm{A}}}{\mathrm{r}^2}\frac{\partial}{\partial\mathrm{r}}\left(\mathrm{r}^2\frac{\partial[\mathrm{A}]}{\partial\mathrm{r}}\right) = 0 \tag{16}$$

$$\frac{\mathrm{D}_{\mathrm{Oil}}^{\mathrm{C}}}{\mathrm{r}^2}\frac{\partial}{\partial\mathrm{r}}\left(\mathrm{r}^2\frac{\partial[\mathrm{C}]}{\partial\mathrm{r}}\right) = 0 \tag{17}$$

Solving equation (16), we get

$$[\mathrm{A}] = -\frac{\gamma_{\mathrm{A}}}{\mathrm{r}} + \delta_{\mathrm{A}} \tag{18}$$

Now as $\mathrm{r} \to \infty$, $[A] \to \mathrm{A}(\infty) = [\mathrm{A}]_{\mathrm{Oil}}^0$, so that $\delta_{\mathrm{A}} = [\mathrm{A}]_{\mathrm{Oil}}^0$

$$\mathrm{A}(\mathrm{r}) = [\mathrm{A}]_{\mathrm{Oil}}^0 - \frac{\gamma_{\mathrm{A}}}{\mathrm{r}} \quad . \tag{19}$$

Similarly for C, from equation (17) we find

$$\mathrm{C}(\mathrm{r}) = [\mathrm{C}]_{\mathrm{Oil}}^0 - \frac{\gamma_{\mathrm{C}}}{\mathrm{r}} \quad . \tag{20}$$

At $r = R$ we have

$$\alpha_{\mathrm{C}}\left([\mathrm{C}]_{\mathrm{Oil}}^0 - \frac{\gamma_{\mathrm{C}}}{\mathrm{R}}\right) = \left[\lambda\zeta^2 + \frac{2\mathrm{n}}{\mathrm{R}}\sinh(\mathrm{R}/\zeta)\right] \tag{21}$$

This gives constant γ_{C} to be

$$\gamma_{\mathrm{C}} = \mathrm{R}[\mathrm{C}]_{\mathrm{Oil}}^0 - \frac{\mathrm{R}\lambda\zeta^2}{\alpha_{\mathrm{C}}} - \frac{2\mathrm{n}}{\alpha_{\mathrm{C}}}\sinh(\mathrm{R}/\zeta) \tag{22}$$

Similarly for A, by matching concentrations at $r = R$ we obtain

$$\begin{aligned}\gamma_{\mathrm{A}} &= \mathrm{R}[\mathrm{A}]_{\mathrm{Oil}}^0 - \frac{\mathrm{qR}}{\alpha_{\mathrm{A}}\mathrm{D}_{\mathrm{IL}}^{\mathrm{A}}} + \frac{\mathrm{R}\mathrm{D}_{\mathrm{IL}}^{\mathrm{C}}}{\alpha_{\mathrm{A}}\mathrm{D}_{\mathrm{IL}}^{\mathrm{A}}}\left[\lambda\zeta^2 + \frac{2\mathrm{n}}{\mathrm{R}}\sinh(\mathrm{R}/\zeta)\right] \\ &= \mathrm{R}[\mathrm{A}]_{\mathrm{Oil}}^0 - \frac{\mathrm{qR}}{\alpha_{\mathrm{A}}\mathrm{D}_{\mathrm{IL}}^{\mathrm{A}}}\left(1 - \frac{\mathrm{K}[\mathrm{B}]_{\mathrm{IL}}^0\,\mathrm{D}_{\mathrm{IL}}^{\mathrm{C}}}{\mathrm{K}[\mathrm{B}]_{\mathrm{IL}}^0\,\mathrm{D}_{\mathrm{IL}}^{\mathrm{C}} + \mathrm{D}_{\mathrm{IL}}^{\mathrm{A}}}\right) + \frac{2\mathrm{n}\mathrm{D}_{\mathrm{IL}}^{\mathrm{C}}\sinh(\mathrm{R}/\zeta)}{\alpha_{\mathrm{A}}\mathrm{D}_{\mathrm{IL}}^{\mathrm{A}}}\end{aligned} \tag{23}$$

Now at steady-state, the fluxes of A and C entering and leaving the interface between the IL and oil have to be equal (assumed no additional specific reactions taking place on the surface). In that case

$$\mathrm{D}_{\mathrm{IL}}^{\mathrm{A}}\left.\frac{\partial[\mathrm{A}]}{\partial\mathrm{r}}\right|_{\mathrm{R}^-} = \mathrm{D}_{\mathrm{Oil}}^{\mathrm{A}}\left.\frac{\partial[\mathrm{A}]}{\partial\mathrm{r}}\right|_{\mathrm{R}^+} \tag{24}$$

and

$$\mathrm{D}_{\mathrm{IL}}^{\mathrm{C}}\left.\frac{\partial[\mathrm{C}]}{\partial\mathrm{r}}\right|_{\mathrm{R}^-} = \mathrm{D}_{\mathrm{Oil}}^{\mathrm{C}}\left.\frac{\partial[\mathrm{C}]}{\partial\mathrm{r}}\right|_{\mathrm{R}^+} \tag{25}$$

where R^- and R^+ refer to two points infinitely close to the interface at each side of the droplet surface in the IL and oil phases, respectively. Substituting equations (14), (15), (19), (20), (22) and (23) into the above equations, and with some rearrangements, we arrive at the following equations:

$$R[A]^0_{Oil}\left(\frac{D^A_{IL}}{D^C_{IL}}\right)-\frac{qR}{\alpha_A D^C_{IL}}+\frac{R}{\alpha_A}\left[\lambda\zeta^2+\frac{2n}{R}\sinh(R/\zeta)\right]=\frac{2nD^A_{IL}}{D^A_{Oil}}\left[\sinh(R/\zeta)-\frac{R}{\zeta}\cosh(R/\zeta)\right]$$

$$-R[C]^0_{Oil}+\frac{R}{\alpha_C}\left(\lambda\zeta^2+\frac{2n}{R}\sinh(R/\zeta)\right)=\frac{2nD^C_{IL}}{D^C_{Oil}}\left[\sinh(R/\zeta)-\frac{R}{\zeta}\cosh(R/\zeta)\right]$$

The above two equations still include the remaining two unknown constants *n* and *q*. These can be determined by solving the above set of simultaneous equations. To do so we first replacing λ from equation (8) in favour of *q* and with further rearrangements we arrive at

$$R[A]^0_{Oil}\left(\frac{D^A_{IL}}{D^C_{IL}}\right)-q\left[\frac{R}{\alpha_A D^C_{IL}}\left(1-\frac{k_1[B]^0_{IL}\zeta^2}{D^A_{IL}}\right)\right]=2n\left[\frac{D^A_{IL}}{D^A_{Oil}}\sinh(R/\zeta)-\frac{1}{\alpha_A}\sinh(R/\zeta)-\frac{RD^A_{IL}}{\zeta D^A_{Oil}}\cosh(R/\zeta)\right]$$

$$-R[C]^0_{Oil}+q\left[\frac{R}{\alpha_C D^A_{IL}}\left(\frac{k_1[B]^0_{IL}\zeta^2}{D^C_{IL}}\right)\right]=2n\left[\frac{D^C_{IL}}{D^C_{Oil}}\sinh(R/\zeta)-\frac{1}{\alpha_C}\sinh(R/\zeta)-\frac{RD^C_{IL}}{\zeta D^C_{Oil}}\cosh(R/\zeta)\right]$$

To simplify the solution we define

$$u_1=R[A]^0_{Oil}\left(\frac{D^A_{IL}}{D^C_{IL}}\right)$$

$$v_1=\frac{R}{\alpha_A D^C_{IL}}\left(1-\frac{k_1[B]^0_{IL}\zeta^2}{D^A_{IL}}\right)$$

$$w_1=2\left[\frac{D^A_{IL}}{D^A_{Oil}}\sinh(R/\zeta)-\frac{1}{\alpha_A}\sinh(R/\zeta)-\frac{RD^A_{IL}}{\zeta D^A_{Oil}}\cosh(R/\zeta)\right]$$

$$u_2=-R[C]^0_{Oil}$$

$$v_2=-\frac{R}{\alpha_C D^A_{IL}}\left(\frac{k_1[B]^0_{IL}\zeta^2}{D^C_{IL}}\right)$$

$$w_2=2\left[\frac{D^C_{IL}}{D^C_{Oil}}\sinh(R/\zeta)-\frac{1}{\alpha_C}\sinh(R/\zeta)-\frac{RD^C_{IL}}{\zeta D^C_{Oil}}\cosh(R/\zeta)\right] \qquad (26)$$

Then the simplified equations can be expressed as

$$u_1-v_1q=w_1n$$

$$u_2-v_2q=w_2n$$

Solving these two equations, we get

$$q=\frac{w_2u_1-w_1u_2}{w_2v_1-w_1v_2}$$

$$n=\frac{u_1}{w_1}-\frac{v_1}{w_1}\left(\frac{w_2u_1-w_1u_2}{w_2v_1-w_1v_2}\right)$$

Now with values of *n*, *q* and therefore also λ (from equation (8)) all known, then taking them into equations (14) and (15), the concentration profiles of reactant A and product C along the droplet radius can be eventually obtained:

$$A(r)=\frac{1}{D_{IL}^{A}}\left(\frac{w_2u_1-w_1u_2}{w_2v_1-w_1v_2}\right)\left(1-\frac{K[B]_{IL}^{0}D_{IL}^{C}}{K[B]_{IL}^{0}D_{IL}^{C}+D_{IL}^{A}}\right) \quad (27)$$
$$-\frac{2D_{IL}^{C}}{rD_{IL}^{A}}\left(\frac{u_1}{w_1}-\frac{v_1}{w_1}\left(\frac{w_2u_1-w_1u_2}{w_2v_1-w_1v_2}\right)\right)\sinh(r/\zeta)$$

$$C(r)=\lambda\zeta^{2}+\frac{2}{r}\left(\frac{u_1}{w_1}-\frac{v_1}{w_1}\left(\frac{w_2u_1-w_1u_2}{w_2v_1-w_1v_2}\right)\right)\sinh(r/\zeta) \quad (28)$$

References

(1) Kong, D. Y.; Zhang, C. M.; Xu, Z. H.; Li, G. G.; Hou, Z. Y.; Lin, J. *J. Colloid Interface Sci.* **2010**, *352*, 278.

(2) Lilly, M. D.; Hornby, W. E.; Crook, E. M. *Biochem. J.* **1966**, *100*, 718.

(3) He, P.; Greenway, G.; Haswell, S. J. *Process Biochem.* **2010**, *45*, 593.

(4) Phan, N. T. S.; Brown，D. H.; Styring, P. A *Green. Chem.* **2004**, *6*, 526.

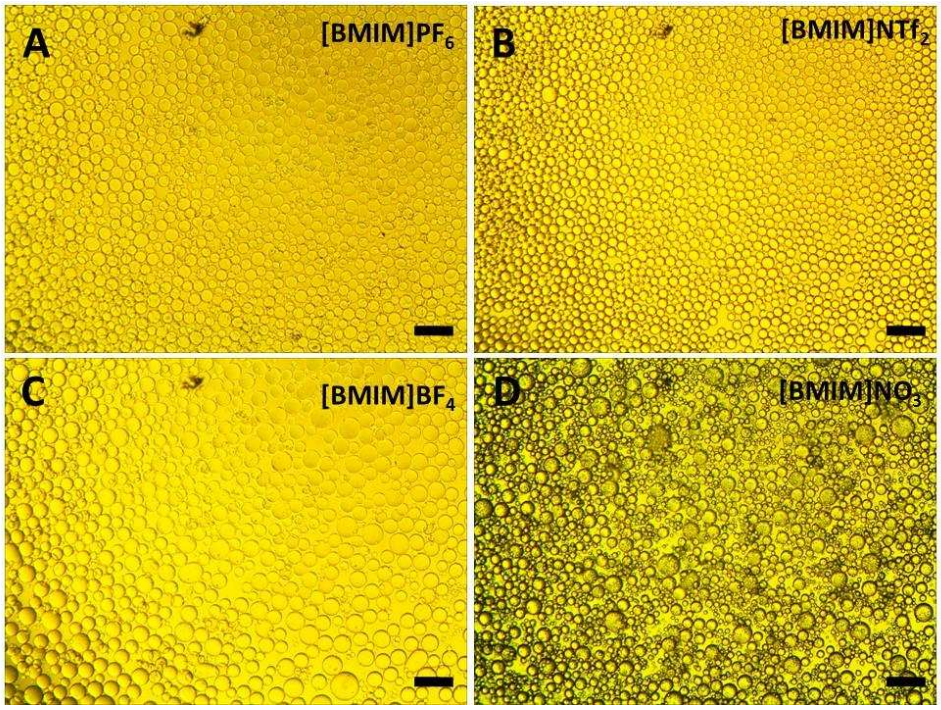

Figure S1. Optical micrographs for the IL-in-octane Pickering emulsions prepared with different ionic liquids. (A) [BMIM]PF_6, (B) [BMIM]NTf_2, (C) [BMIM]BF_4, (D) [BMIM]NO_3. The emulsions consist of 2.4 mL *n*-octane, 4.7 mL ionic liquid, 80 μL enzyme solution (4 mg mL^{-1} of protein; pH 8.0) and 0.195 g emulsifier. Scale bar = 100 μm.

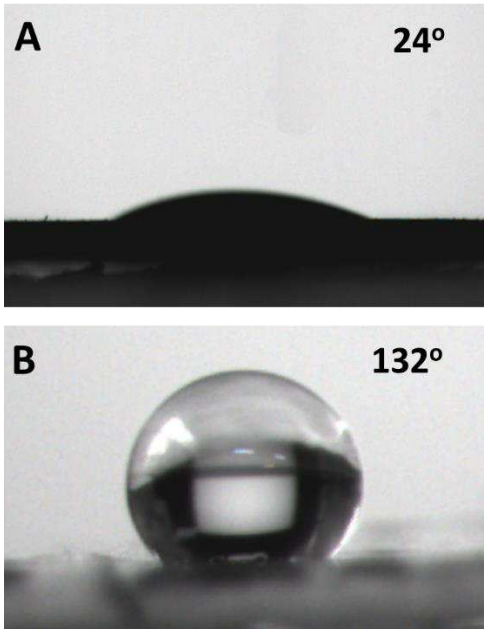

Figure S2. Appearance of a water droplet in air on a disk of compressed silica particles. (A) unmodified silica and (B) hydrophobically modified silica.

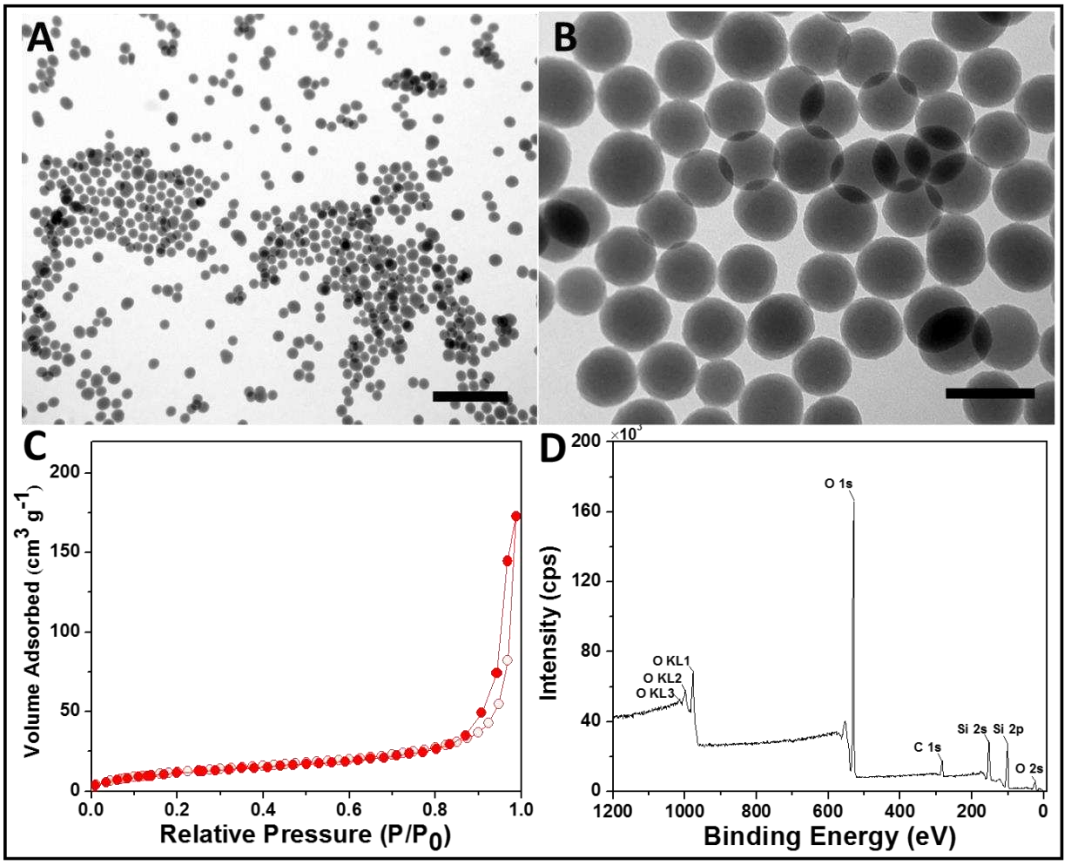

Figure S3. Characterization of silica particle emulsifier. (A) TEM image, scale bar = 500 nm; (B) higher magnification TEM image, scale bar = 100 nm; (C) N_2 adsorption (open points)–desorption (filled points) isotherms. Specific surface area is 47 m^2 g^{-1}; (D) X-Ray photoelectron spectrum. According to the results of elemental analysis, the loading of dimethyldichlorosilane on silica was estimated as 1.14 mmol g^{-1}.

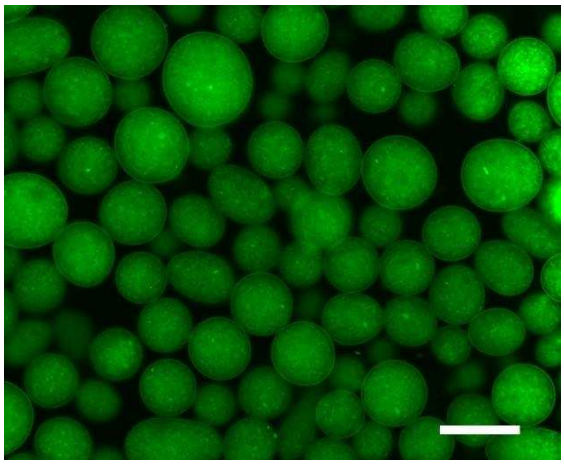

Figure S4. Fluorescence confocal microscopy image for the IL-in-octane Pickering emulsion with the IL dyed with FITC-I. Scale bar = 100 μm. The emulsion consists of 2 g [BMIM]PF_6 labeled with FITC-I (2 μM), 0.7 mL *n*-octane and 0.06 g solid emulsifier.

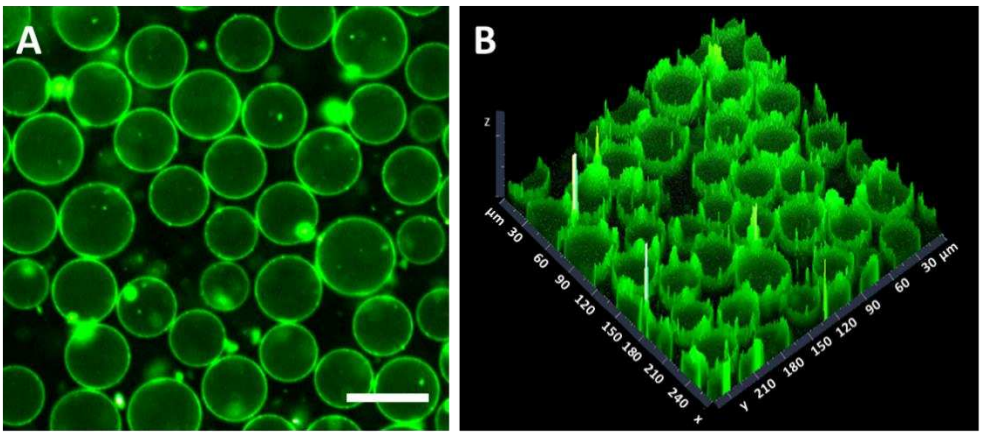

Figure S5. Fluorescence confocal microscopy image of the IL-in-toluene Pickering emulsion with the emulsifier dyed with FITC-I. (A) 2D fluorescence confocal microscopy image, scale bar = 50 μm; (B) 3D fluorescence confocal microscopy image. The emulsion consists of 2 g [BMIM]PF_6, 0.7 mL toluene and 0.06 g solid emulsifier labeled with FITC-I.

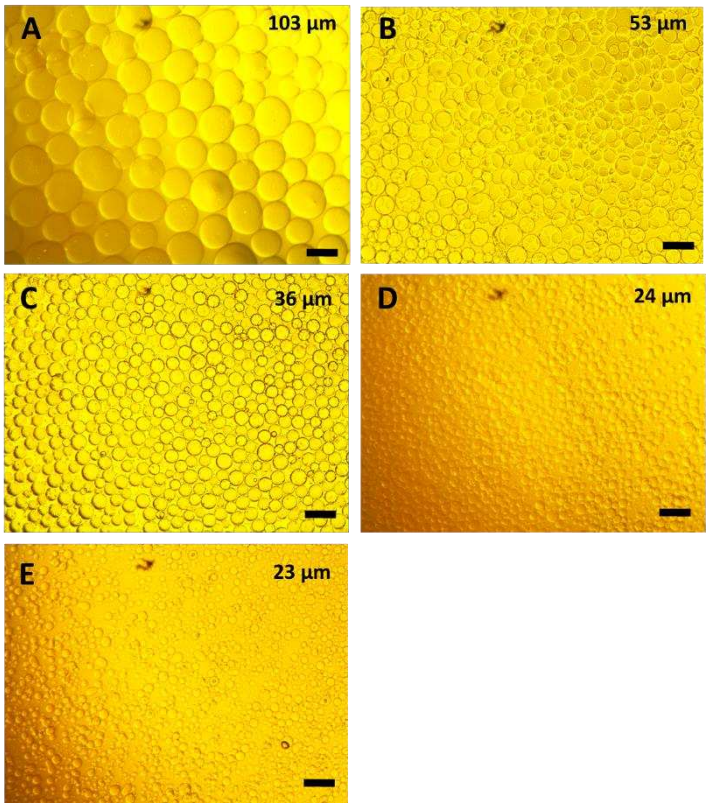

Figure S6. Optical micrographs for the IL-in-octane Pickering emulsions of different droplet sizes. Scale bar = 100 μm. The emulsions consist of 6.5 g [BMIM]PF_6, 2.4 mL *n*-octane and different amounts of solid emulsifier (with respect to IL): (a) 1 wt %, (b) 2 wt %, (c) 3 wt %, (d) 4 wt %, (e) 5 wt %.

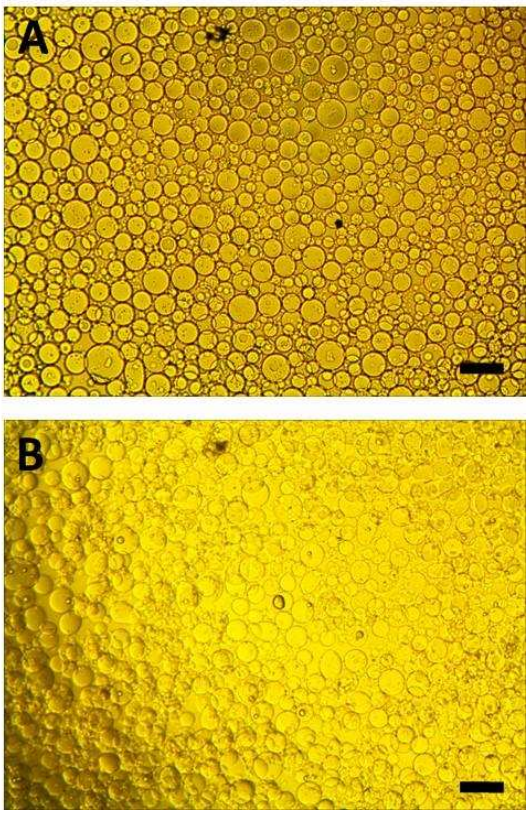

Figure S7. Optical micrographs for the IL-in-octane Pickering emulsions before and after 72 h of flowing at 100 °C. (A) Before flowing, (B) after flowing for 72 h, Scale bar = 100 μm. The emulsion consists of 6.5 g [BMIM]PF_6, 2.4 mL *n*-octane and 0.195 g solid emulsifier.

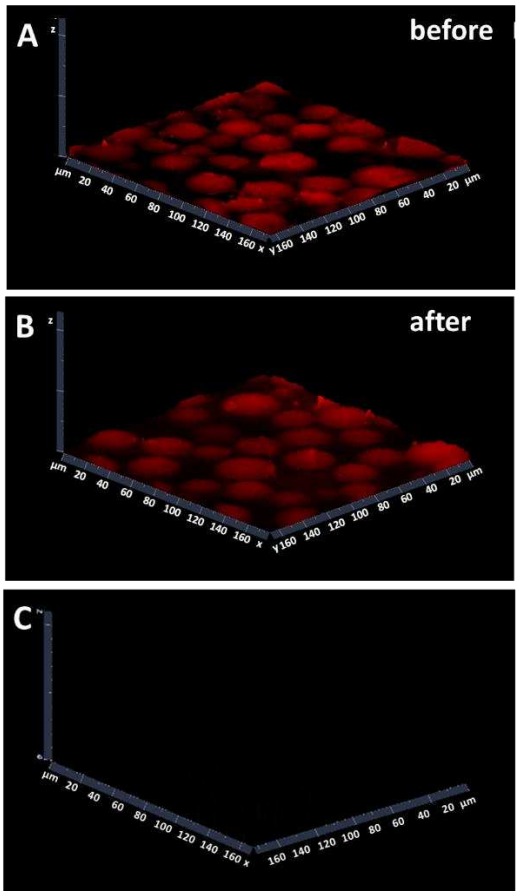

Figure S8. 3D fluorescence confocal microscopy images for the Rhodamine B-labeled enzyme within droplets before and after 48 h of flowing. (A) Before flowing, (B) after flowing for 48 h, (C) fluorescence confocal microscopy image of the effluent oil phase after 48 h, flow rate = 5 mL h^{-1}. The IL-in-oil Pickering emulsion consists of 2 g [BMIM]PF_6, 0.7 mL *n*-octane, 0.06 g emulsifier and 30 μL of the solution of Rhodamine B-labeled emzyme in PBS (30 mg mL^{-1}).

Note: The average fluorescence intensity within droplets was 247 initially and 246 after flowing for 48 h.

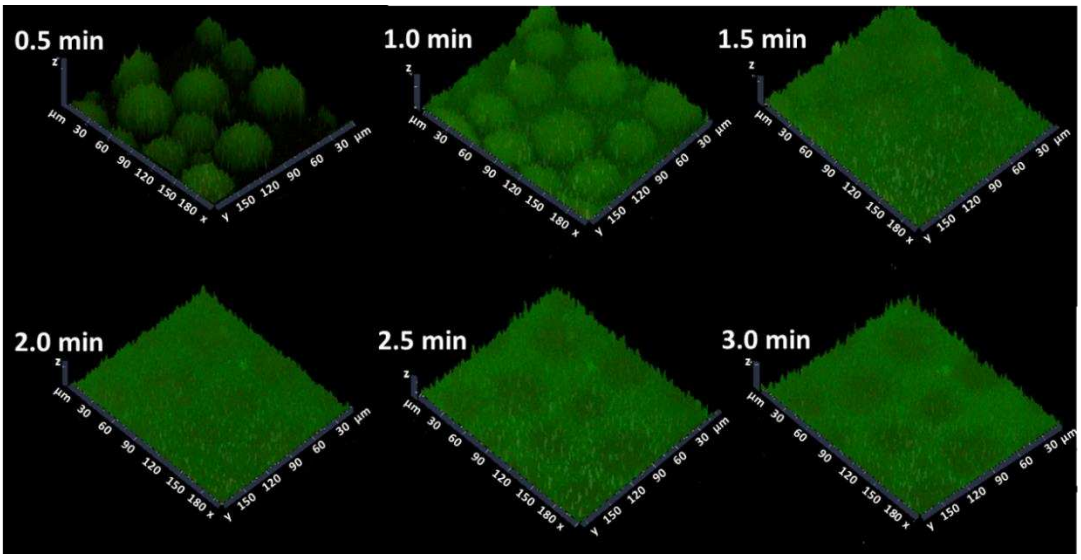

Figure S9. 3D fluorescence confocal microscopy image for the transport of FITC-I out of IL droplets for various times. The IL-in-octane Pickering emulsion consists of 2 g [BMIM]PF_6, 0.7 mL *n*-octane and 0.06 g solid emulsifier.

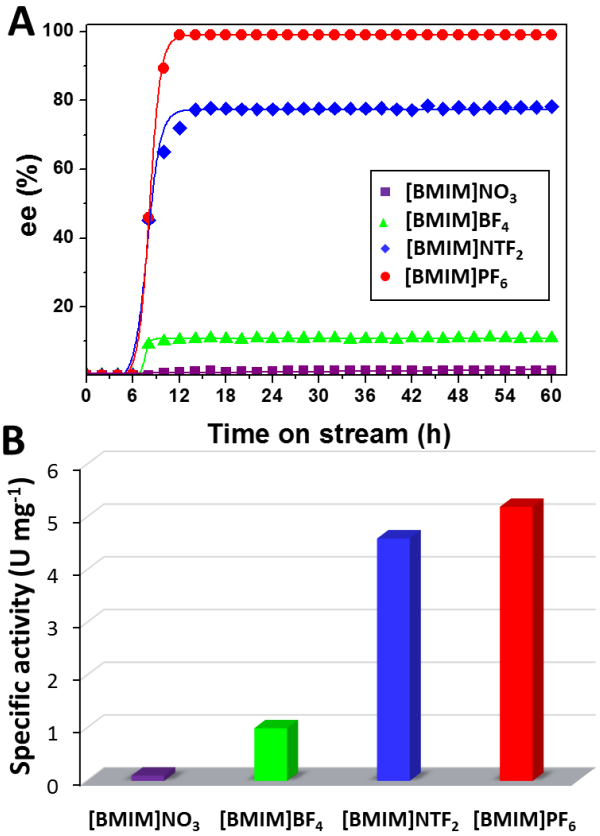

Figure S10. CALB-catalyzed enantioselective trans-esterification of 1-phenylethyl alcohol in the continuous flow systems using different ILs. (A) Enantiomeric excess (ee%) *vs* time, (B) specific activity for various ILs. The IL-in-octane Pickering emulsions consist of 2.4 mL *n*-octane, 4.7 mL ionic liquid, 80 μL aqueous enzyme solution (4 mg mL^{-1} of protein; pH 8.0) and 0.195 g emulsifier. Reaction conditions: a solution of 1-phenylethyl alcohol (0.1 M) and vinyl acetate (0.4 M) in *n*-octane as mobile phase, 45 °C, flow rate = 2 mL h^{-1}.

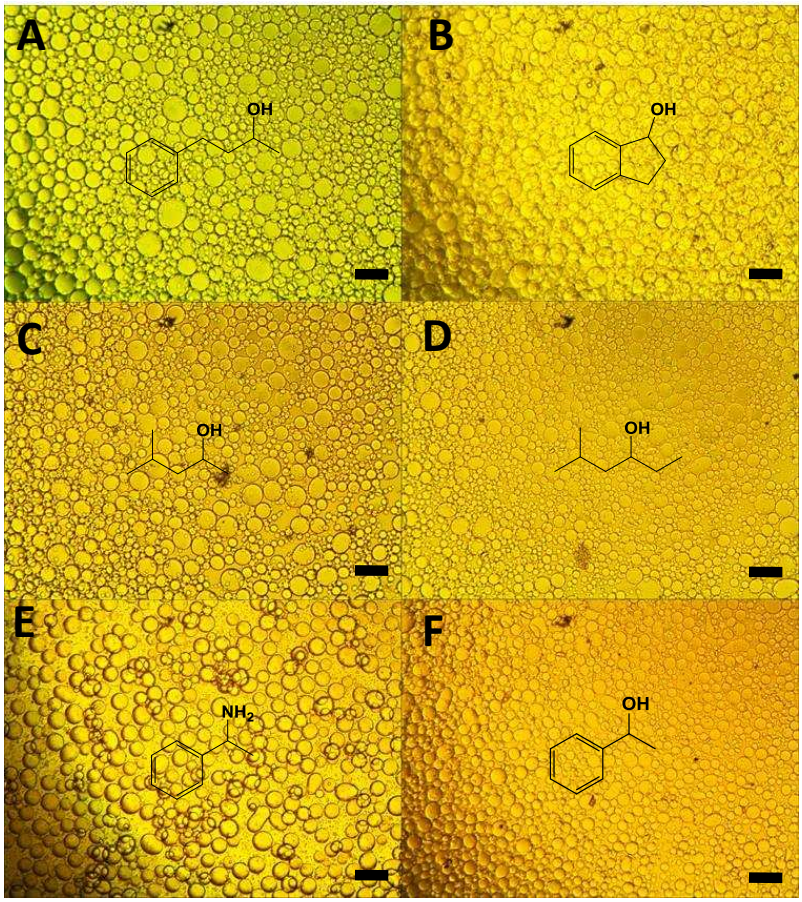

Figure S11. Optical micrographs of IL droplets after enzymatic reactions. Scale bar = 100 μm. (A) Enantioselective trans-esterification of 4-phenyl-2-butanol and vinyl acetate after 720 h, (B) enantioselective trans-esterification of 1-indanol and vinyl acetate after 720 h, (C) enantioselective trans-esterification of 4-methyl-2-pentanol and vinyl acetate after 720 h, (D) enantioselective trans-esterification of 5-methyl-3-hexanol and vinyl acetate after 720 h, (E) enantioselective amidation of 1-phenylethylamine and ethyl methoxyacetate after 720 h, (F) enantioselective trans-esterification of 1-phenylethyl alcohol and vinyl acetate after 4000 h. Emulsion composition and reaction conditions are included in Figure 3 in main text.

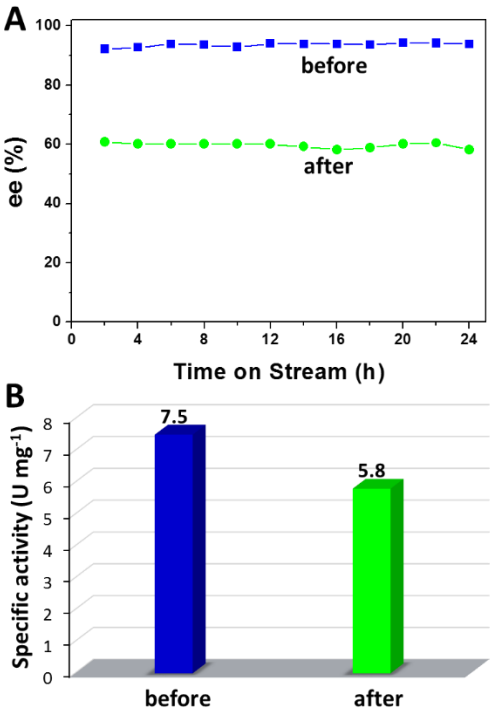

Figure S12. Comparison of the specific activity of CALB in the IL-based flow system before and after 4000 h on stream. (A) Enantiomeric excess values of 1-phenylethyl alcohol against time before and after 4000 h on stream, flow rate = 3 mL h^{-1}; (B) Specific activity of CALB before and after 4000 h on stream. The IL-in-octane Pickering emulsion consists of 80 μL aqueous enzyme solution (4 mg mL^{-1} of protein; pH 8.0), 6.5 g [BMIM]PF_6, 2.4 mL *n*-octane and 0.195 g solid emulsifier.

Note: After 4000 h on stream, 77% of the initial specific activity of CALB was still maintained.

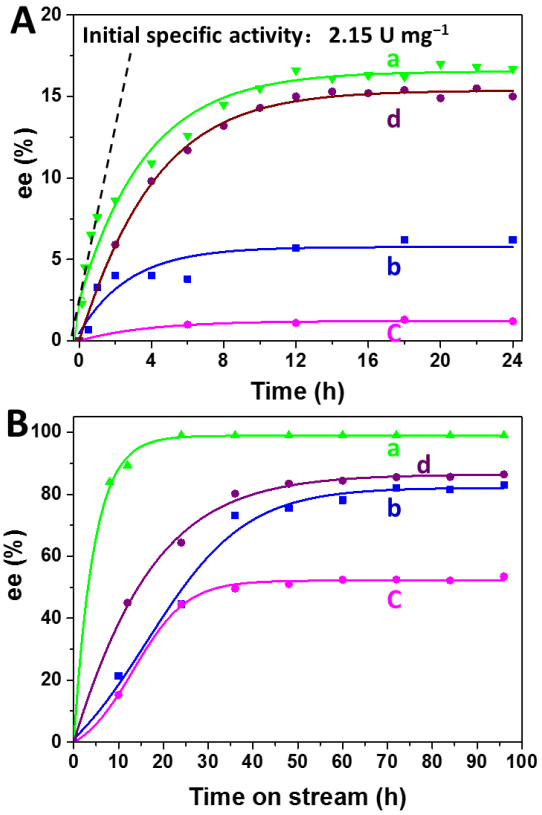

Figure S13. Kinetic profiles for the CALB-catalyzed enantioselective trans-esterification and amidation in batch and IL droplet-based flow system. (A) Enantiomeric excess (ee%) *vs* time in the batch system, (B) enantiomeric excess (ee%) *vs* time in the IL droplet-based flow system. The racemic alcohols and amine used in the reactions are: (a) 1-phenylethyl alcohol, (b) 5-methyl-3-hexanol, (c) 1-phenyl-1-propanol, (d) 1-phenylethylamine, respectively. Batch reaction conditions: 2 g [BMIM]PF_6 containing 25 μL (for alcohols) or 75 μL (for amine) aqueous enzyme solution (4 mg mL^{-1} of protein; pH 8.0), 1 mL *n*-octane or toluene containing racemic alcohols (0.1 M) or racemic amine (0.05 M) and vinyl acetate (for alcohols, 0.4 M) or ethyl methoxyacetate (for amine, 0.2 M), 45 °C, 2600 rpm. The initial specific activity is calculated at the beginning of reaction (within 20 min). Flow systems: the IL-based Pickering emulsions consist of 80 μL (for alcohols) or 240 μL (for amine) aqueous enzyme solution (4 mg mL^{-1} of protein; pH 8.0), 6.5 g [BMIM]PF_6, 2.4 mL *n*-octane or toluene and 0.195 g emulsifier, mobile phase is a solution of racemic alcohol (0.1 M) or racemic amine (0.05 M) and vinyl acetate (for alcohols, 0.4 M) or ethyl methoxyacetate (for amine, 0.2 M) in *n*-octane or toluene, 45 °C, flow rate = 2 mL h^{-1} for 1-phenylethyl alcohol, 0.25 mL h^{-1} for 5-methyl-3-hexanol, 0.25 mL h^{-1} for 1-phenyl-1-propanol, 0.5 mL h^{-1} for 1-phenylethylamine.

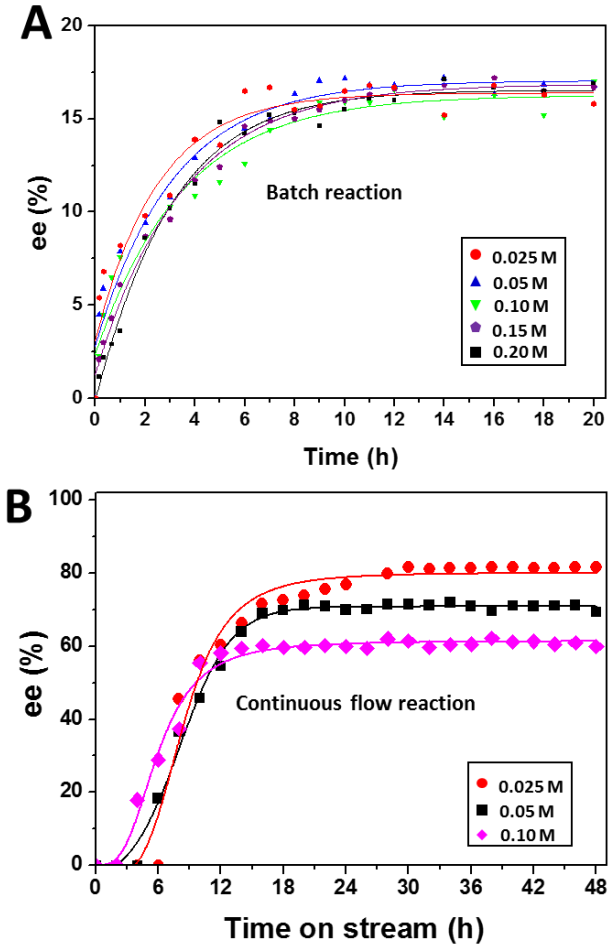

Figure S14. Kinetic profiles for the CALB-catalyzed enantioselective trans-esterification in batch and IL droplet-based flow system using different concentrations of 1-phenylethyl alcohol. (A) Batch reaction system, (B) IL droplet-based flow catalysis system. Batch reaction conditions: 2 g of [BMIM]PF_6 containing 25 μL aqueous enzyme solution (4 mg mL^{-1} of protein; pH 8.0), 1 mL of *n*-octane containing a given concentration of 1-phenylethyl alcohol and vinyl acetate (molar ratio = 1:4), 2600 rpm, 45 °C. Flow systems: the IL-based Pickering emulsions consist of 6.5 g [BMIM]PF_6, 2.4 mL *n*-octane, 80 μL aqueous enzyme solution (4 mg mL^{-1} of protein; pH 8.0) and 0.195 g emulsifier. The mobile phase was a solution of a given concentration of 1-phenylethyl alcohol and vinyl acetate in *n*-octane (molar ratio = 1:4), flow rate = 5 mL h^{-1}.

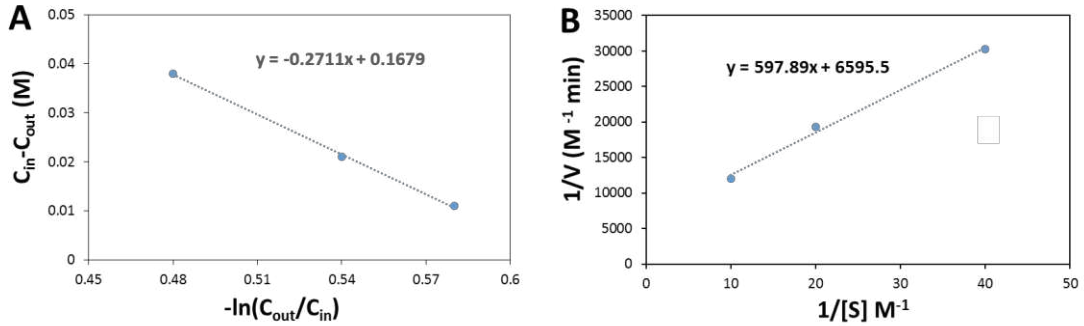

Figure S15. Lilly–Hornby plot and Lineweaver-Burk plot. (A) Lilly–Hornby plot obtained for the continuous flow reaction, flow rate = 5 mL h^{-1}; (B) Lineweaver-Burk plot obtained for the batch reaction, 2600 rpm.

Notes: Kinetic constants for the CALB in the IL-based flow reaction were obtained from the Lilly-Hornby model, which was developed for the packed-bed reaction system.[2,3]

$$C_{in} - C_{out} = K_m \ln \frac{C_{out}}{C_{in}} + \frac{V_{max} V_{void}}{Q}$$

where C_{in} and C_{out} are the reactant concentrations at the inlet and at the outlet, V_{void} is the void volume of the packed column, Q is the flow rate, K_m is the apparent Michaelis constant obtained from the slope of the plot, V_{max} is the maximal reaction rate calculated from the Y-axis intercept and the turnover number k_{cat} was calculated by V_{max}/[lipase].

The kinetic parameters Michaelis constant K_m and the maximum reaction rate V_{max} were calculated using the Lineweaver-Burk equation[2]:

$$\frac{1}{v} = \frac{K_m}{V_{max}[S]} + \frac{1}{V_{max}}$$

where v is the initial reaction rate, V_{max} is the maximal reaction rate and [S] is the concentration of the substrate.

Comparison of K_m, V_{max} and k_{cat} between batch and IL droplet-based continuous flow reactions

	K_m (M)	V_{max} (M min^{-1})	k_{cat} (min^{-1})
Continuous flow reaction	0.27	5.8×10^{-3}	3.9×10^{3}
Batch reaction	0.26	8.5×10^{-4}	8.5×10^{2}

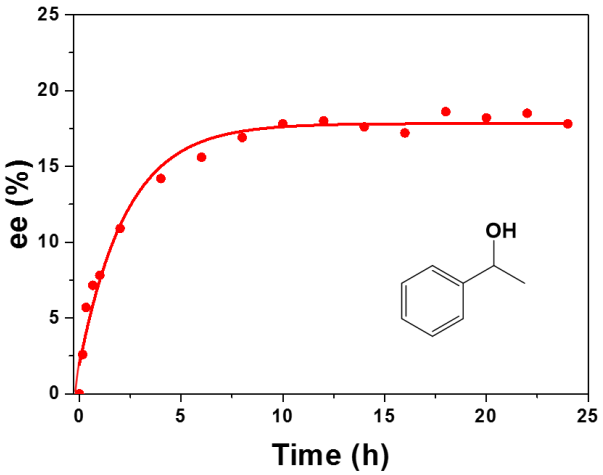

Figure S16. Kinetic profiles for CALB-catalyzed enantioselective trans-esterification of 1-phenylethyl alcohol in an IL droplet-based system **without flow.** Other reaction conditions are the same as those of the IL-droplet-based flow system (Figure S13B, a) **except no flow**.

Notes: The specific activity of CALB in the IL droplet-based system without flow is determined to be 0.25 U mg^{-1}, according to the ee value within the first 600 min. This value is 1/21 of the specific activity in the flow system. These comparisons confirm that the flow enhances the specific activity of the enzymatic reaction even at low conversion.

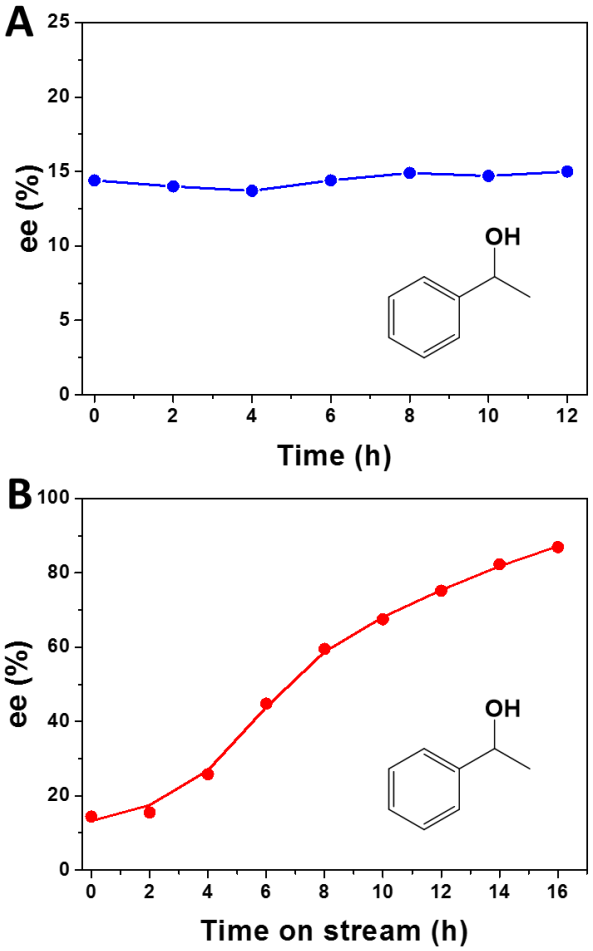

Figure S17. Kinetic profiles for CALB-catalyzed enantioselective trans-esterification of 1-phenylethyl alcohol in a batch system and in an IL droplet-based flow system, **where the product** (*R*)-1-phenethyl acetate **was introduced before reaction**. (A) Enantiomeric excess (ee%) *vs* time in the batch system, (B) enantiomeric excess (ee%) *vs* time in the IL droplet-based flow system. Batch reaction conditions: 2 g [BMIM]PF_6 containing 25 μL aqueous enzyme solution (4 mg mL^{-1} of protein; pH 8.0), 1 mL *n*-octane containing 1-phenylethyl alcohol (0.1 M), vinyl acetate (0.4 M) and **(*R*)-1-phenethyl acetate** (**product**, 0.012 M), 45 °C, 2600 rpm. IL droplet-based system: IL-based Pickering emulsion consists of 80 μL aqueous enzyme solution (4 mg mL^{-1} of protein; pH 8.0), 6.5 g [BMIM]PF_6, 2.4 mL *n*-octane and 0.195 g emulsifier, mobile phase is a solution of 1-phenylethyl alcohol (0.1 M), vinyl acetate (0.4 M) and **(*R*)-1-phenethyl acetate** (**product**, 0.012 M) in *n*-octane, 45 °C, flow rate = 2 mL h^{-1}.

Notes: In the batch reaction, the ee value of 1-phenylethyl alcohol does not increase with time, indicating no reaction, caused by the product inhibition effect even at low conversion. In contrast, in the IL droplet-based flow system, the ee value gradually increases, suggesting that the flow system can indeed mitigate the product inhibition effect.

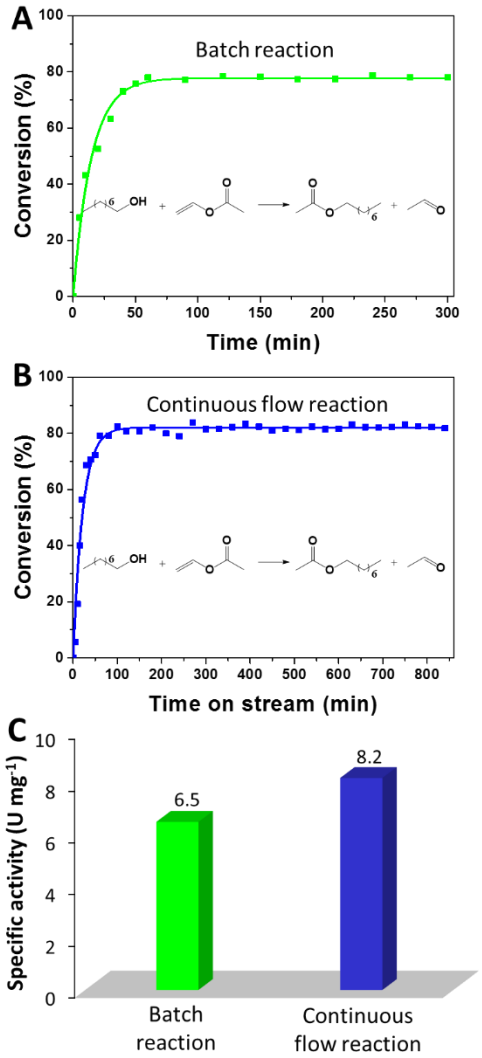

Figure S18. Comparison of CALB-catalyzed trans-esterification of 1-octanol and vinyl acetate in a batch system and in an IL droplet-based flow system, where **this reaction does not suffer from the severe product inhibition effect** since the conversion in the batch reaction can reach 80%. (A) Conversion *vs* time in the batch system, (B) conversion *vs* time in the IL droplet-based flow system, (C) specific activity of CALB in both systems. Specific activity of CALB for the batch system is calculated within the first 60 min. Specific activity of CALB for the IL droplet-based flow reactions is calculated at steady state. Batch reaction conditions: 2 g [BMIM]PF_6 containing 50 μL aqueous enzyme solution (4 mg mL^{-1} of protein; pH 8.0), 1 mL *n*-octane containing 1-octanol (0.1 M) and vinyl acetate (0.15 M), 45 °C, 2600 rpm. IL droplet-based flow system: IL-based Pickering emulsion consists of 50 μL aqueous enzyme solution (4 mg mL^{-1} of protein; pH 8.0), 2 g [BMIM]PF_6, 0.7 mL *n*-octane and 0.06 g emulsifier, mobile phase is a solution of 1-octanol (0.1 M) and vinyl acetate (0.15 M) in *n*-octane, 45 °C, flow rate = 1.2 mL h^{-1}.

Notes: Specific activity of CALB in the batch system and in the IL droplet-based flow system are 6.5 and 8.2 U mg^{-1}, respectively. For this enzymatic reaction without severe product inhibition effects, the specific activity for these two system is close, rather than 1/21 in the case of the enzymatic reaction suffering from product inhibition effects.

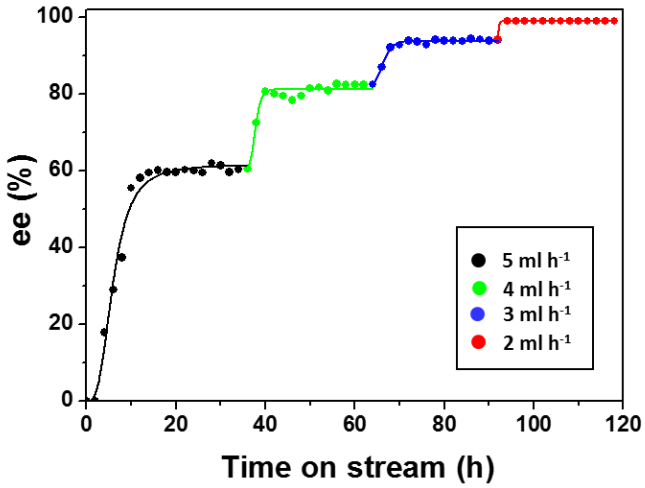

Figure S19. Kinetic profile for the CALB-catalyzed enantioselective trans-esterification of 1-phenylethyl alcohol in the IL droplet-based flow system at different flow rates. The IL-in-octane Pickering emulsion consists of 6.5 g [BMIM]PF_6, 2.4 mL *n*-octane, 80 μL aqueous enzyme solution (4 mg mL^{-1} of protein; pH 8.0) and 0.195 g emulsifier. The mobile phase was a solution of 1-phenylethyl alcohol (0.1 M) and vinyl acetate (0.4 M) in *n*-octane, 45 °C.

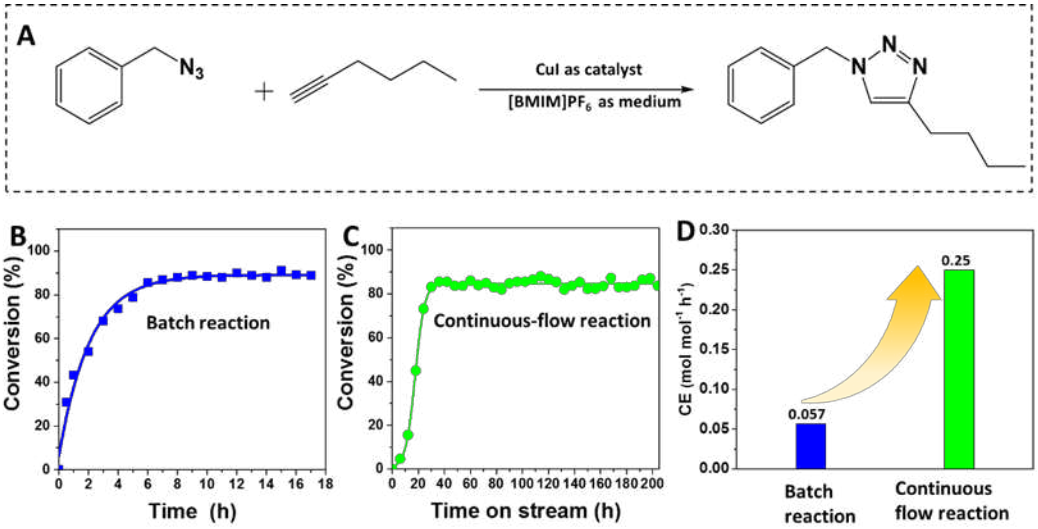

Figure S20. CuI-catalyzed cycloaddition of benzyl azide and 1-hexyne in batch and in IL droplet-based flow system. (A) Cycloaddition of benzyl azide and 1-hexyne, (B) kinetic profile for the cycloaddtion in the batch system, (C) conversions with time for the cycloaddtion in the IL droplet-based flow system, (D) catalysis efficiency (CE) of CuI in the batch system and in the IL droplet-based flow system. For the batch system, the CE is calculated according to the conversion within the first 9 h. For the flow system, the CE is calculated after the conversion levelled off (at steady state). Batch reaction conditions: 2 g [BMIM]PF_6, 0.032 g CuI, 0.16 g L-ascorbic acid sodium (as antioxidant), 1 mL solution of benzyl azide (0.1 M) and 1-hexyne (0.12 M) in a mixture of *n*-octane and toluene (v/v = 1:1), 25 °C, 2600 rpm. Continuous flow reaction conditions: the IL-in-oil Pickering emulsion consists of 2 g [BMIM]PF_6, 0.032 g CuI, 0.16 g L-ascorbic acid sodium, 0.7 mL of a mixture of *n*-octane and toluene (v/v = 1:1) and 0.06 g emulsifier, mobile phase is a solution of benzyl azide (0.1 M) and 1-hexyne (0.12 M) in a mixture of *n*-octane and toluene (v/v = 1:1), 25 °C, flow rate from initial 0.5 mL h^{-1} to 0.35 mL h^{-1} at the end.

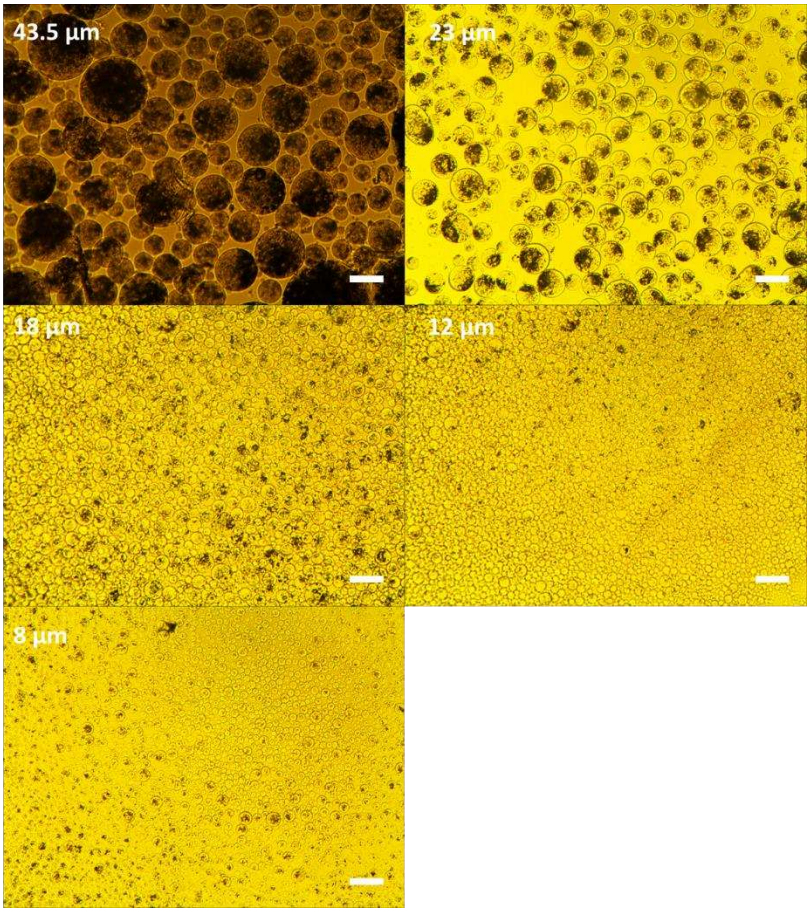

Figure S21. Optical micrographs of IL-in-oil Pickering emulsions containing CuI with different droplet radii. Scale bar = 100 μm. The emulsions consist of 2 g [BMIM]PF_6, 0.032 g CuI, 0.16 g L-ascorbic acid sodium (as antioxidant), 0.7 mL of a mixture of *n*-octane and toluene (v/v = 1:1), and the amount of solid emulsifier (with respect to the ionic liquid) is 1 wt %, 2 wt %, 3 wt %, 4 wt % and 5 wt %.

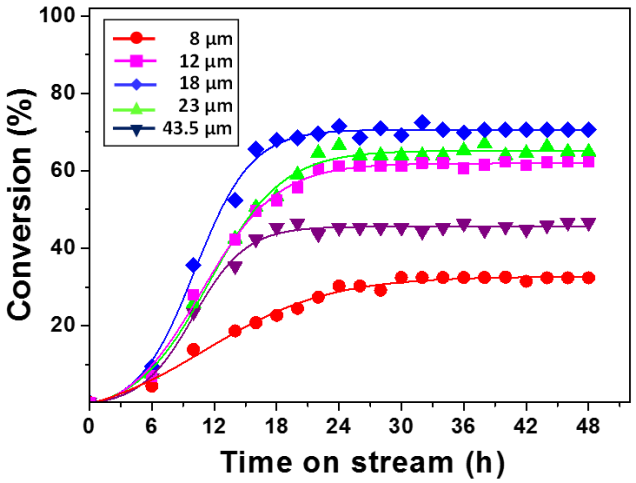

Figure S22. Conversions with time for CuI-catalyzed cycloaddition of benzyl azide and phenyl acetylene in the flow systems using different droplet radii. The IL-in-oil Pickering emulsion consist of 2 g [BMIM]PF_6, 0.032 g CuI, 0.16 g L-ascorbic acid sodium (as antioxidant), 0.7 mL of a mixture of *n*-octane and toluene (v/v = 1:1), and the amount of solid emulsifier (with respect to the ionic liquid) is 1 wt %, 2 wt %, 3 wt %, 4 wt % and 5 wt %. The mobile phase was a solution of benzyl azide (0.1 M) and phenyl acetylene (0.12 M) in a mixture of *n*-octane and toluene (v/v = 1:1), 25 °C, flow rate = 1.5 mL h^{-1}.

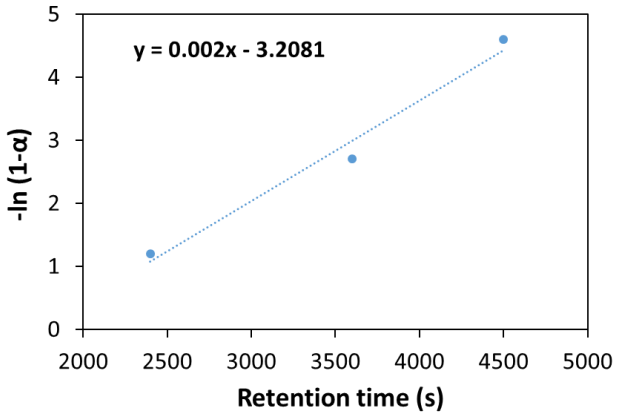

Figure S23. Kinetic plot for the determination of the observed rate constant for CuI-catalyzed cycloaddition in the continuous flow system.

Notes: Considering that the cycloaddition reaction is a first-order process and the equation for packed bed reactor is given as: [4]

$$-ln(1-\alpha) = k_{obs}t$$

where α is the mole fraction of 1-benzyl-4-phenyl-1,2,3-triazole produced and t is the corresponding reaction time. The slope of the plot of $-ln(1-\alpha)$ *vs* t yields the value of the observed rate constant for the continuous flow reaction, i.e. $k_{obs} = k_1 B_{IL}^0$. Therefore, the rate constant of the backward reaction k_2 can also be estimated according to the reaction equilibrium constant K. The detailed experimental data for the CuI-catalyzed cycloaddition of benzyl azide and phenyl acetylene in the IL droplet-based flow system at different flow rates are listed below.

In this reaction, the equation of $\zeta^{-2} = (k_1 B_{IL}^0 / D_{IL}^A) + (k_2 / D_{IL}^C)$ can be simplified to $\zeta^{-2} = k_1 B_{IL}^0 / D_{IL}^A$, since $k_2 << k_1$. Taking the value of the observed rate constant $k_{obs} = k_1 = 2\times10^{-3}$ s^{-1} in the above equation, the thickness ζ can be estimated as 15.8 μm.

Results of the CuI-catalyzed cycloaddition in the IL droplet-based flow system at different flow rates

Flow rate (mL h^{-1})	0.8	1	1.5
Retention time (s)	4500	3600	2400
Conversion levelled off (%)	>99	93	70
$-ln(1-\alpha)$	4.6	2.7	1.2

Mass Spectrometry Spectra

For CALB-Catalyzed Enantioselective Trans-Esterification:

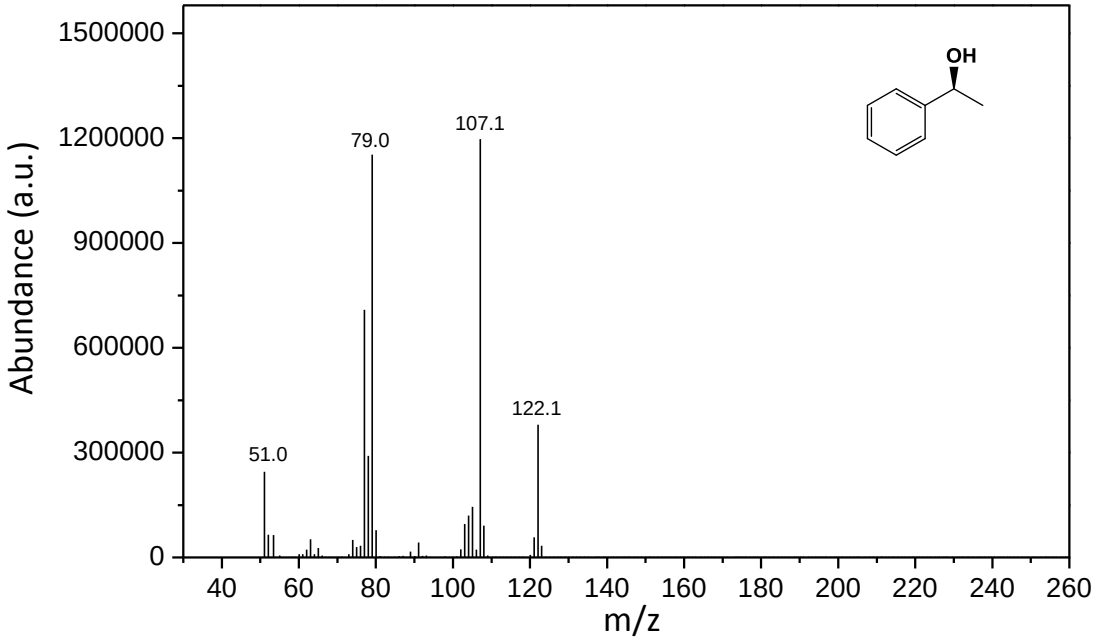

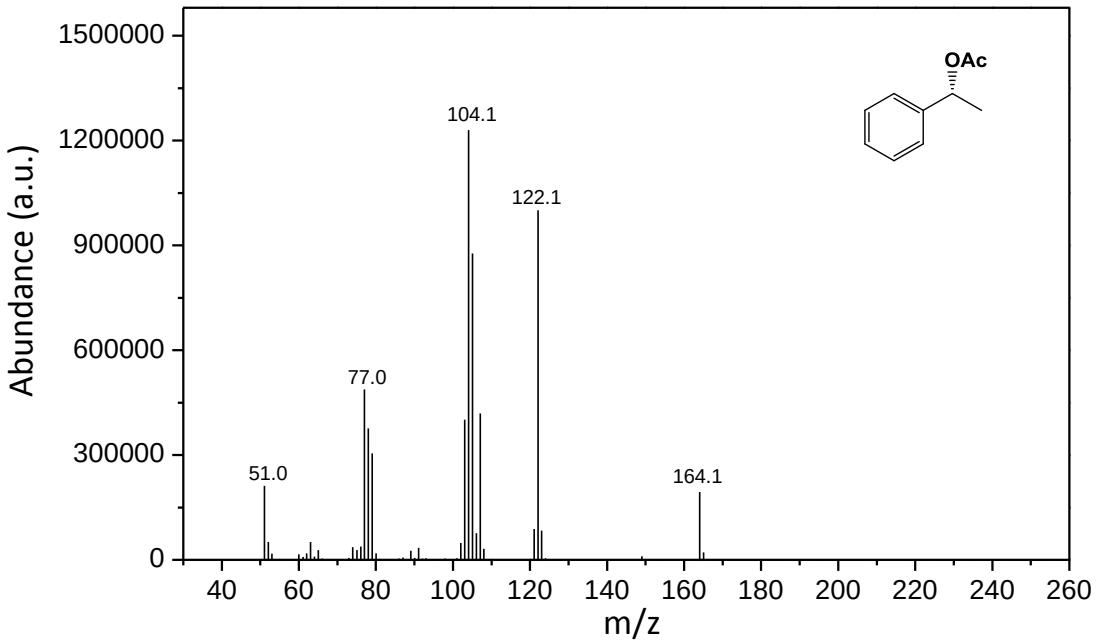

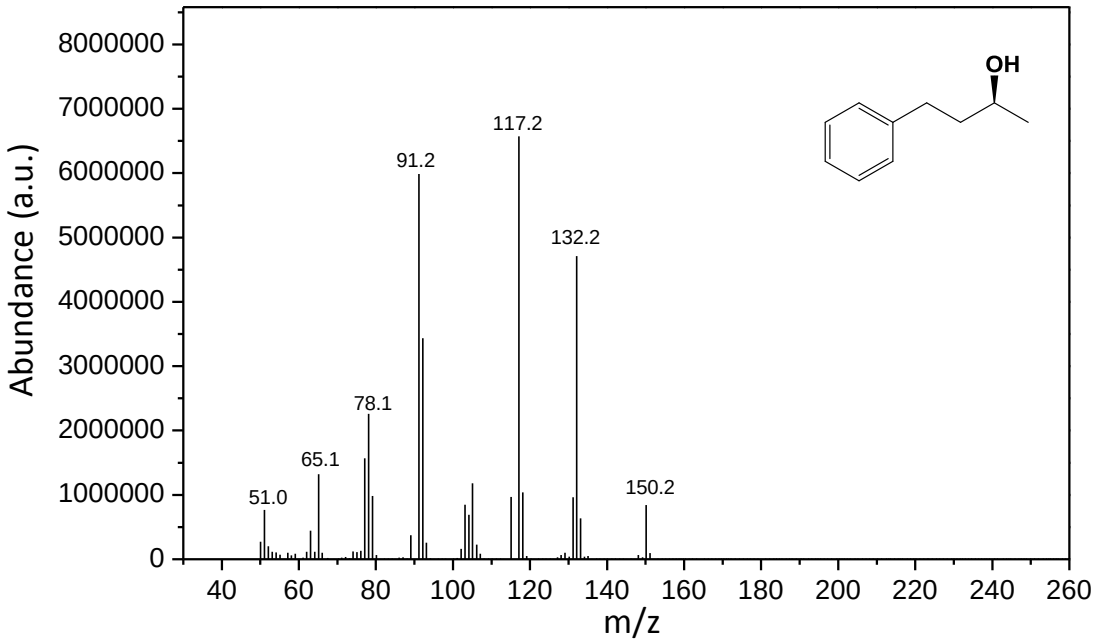
Abundance (a.u.)
m/z
OH
117.2
91.2
132.2
78.1
65.1
51.0
150.2

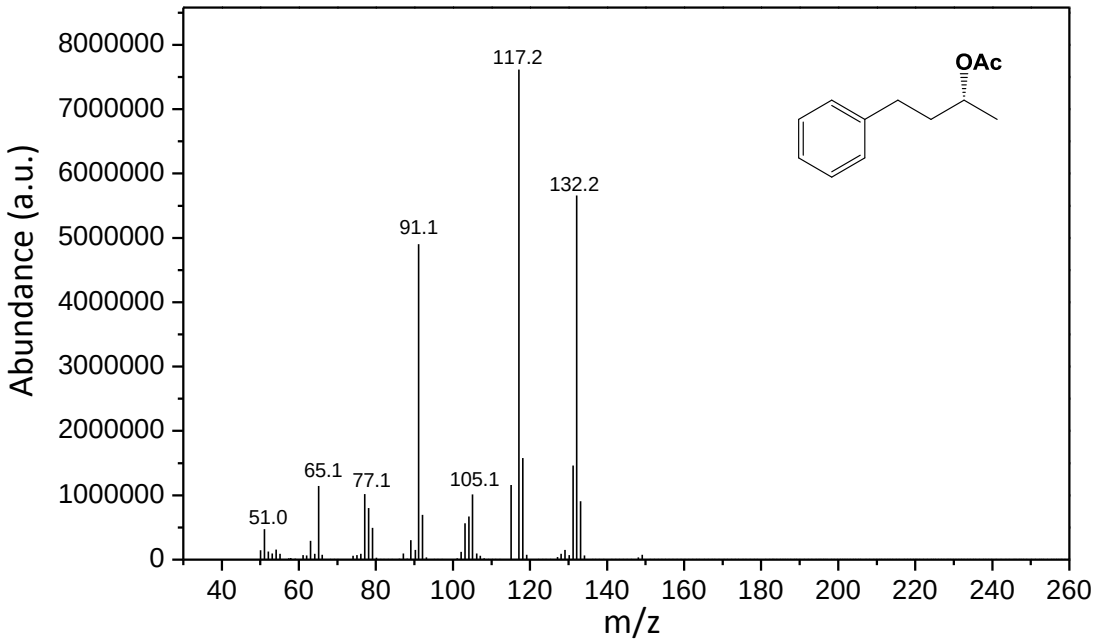
Abundance (a.u.)
m/z
OAc
117.2
132.2
91.1
65.1
77.1
105.1
51.0

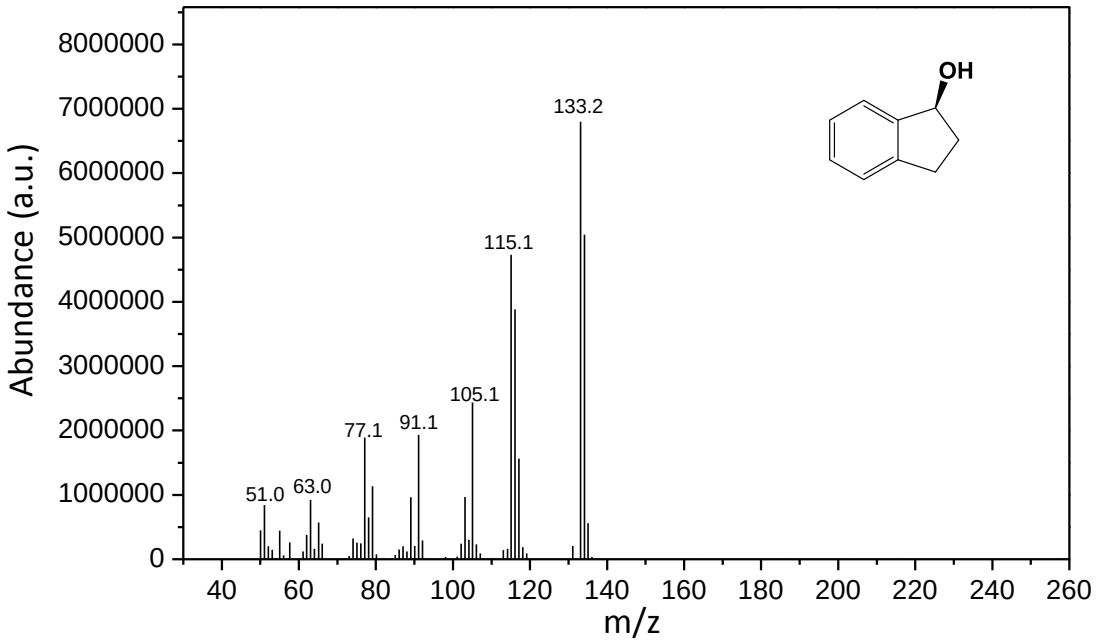
Abundance (a.u.)
m/z
OH
133.2
115.1
105.1
91.1
77.1
63.0
51.0

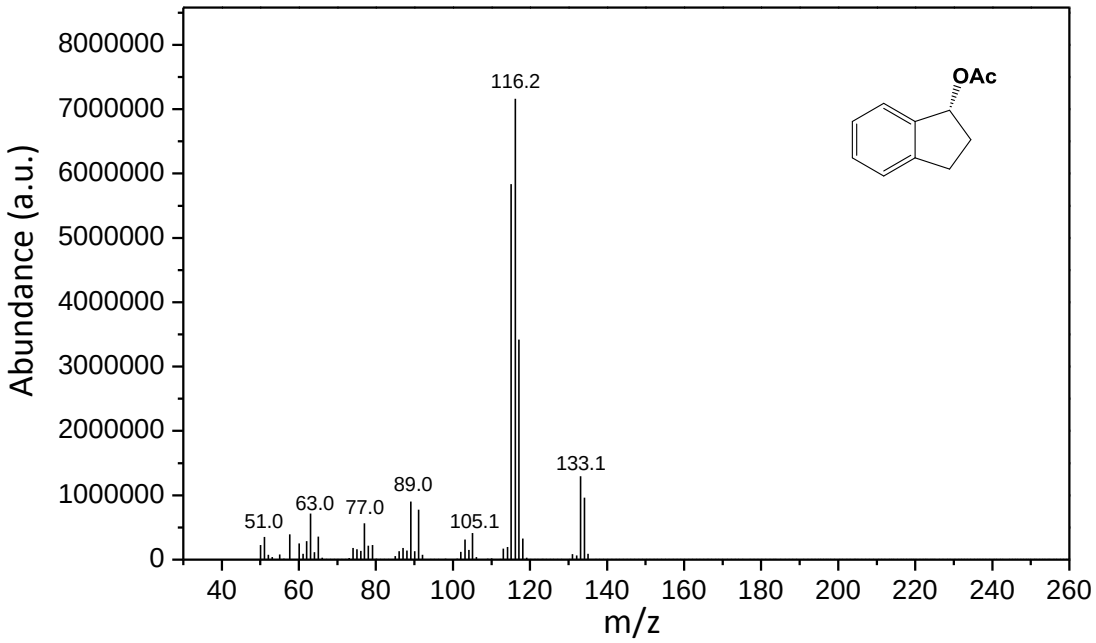
Abundance (a.u.)
m/z
OAc
116.2
133.1
89.0
63.0
77.0
51.0
105.1

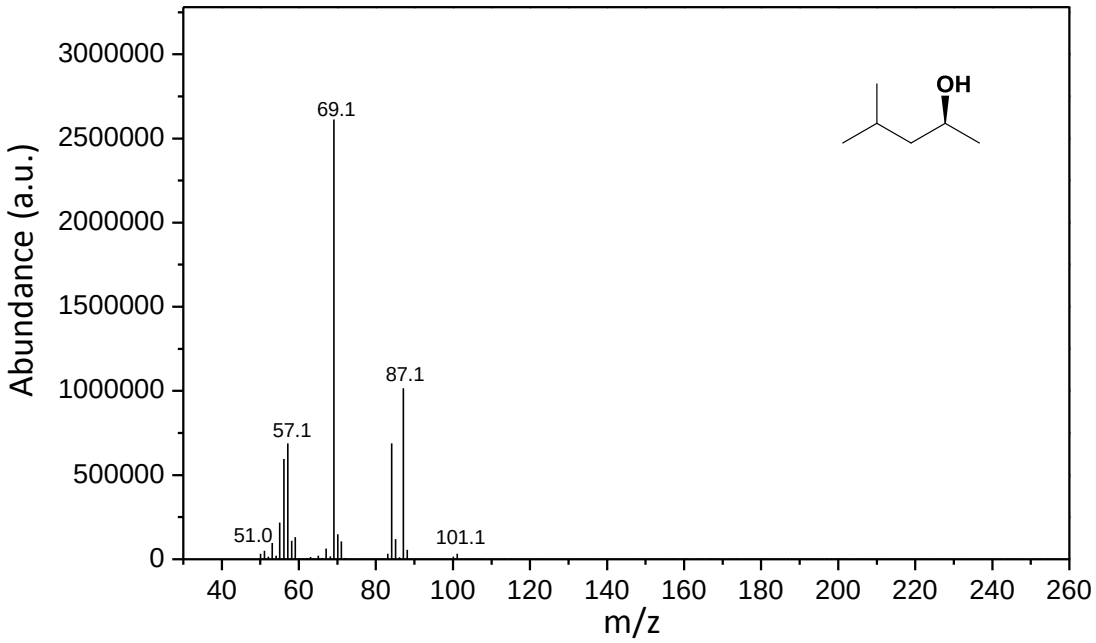
Abundance (a.u.)
m/z
OH
69.1
87.1
57.1
51.0
101.1

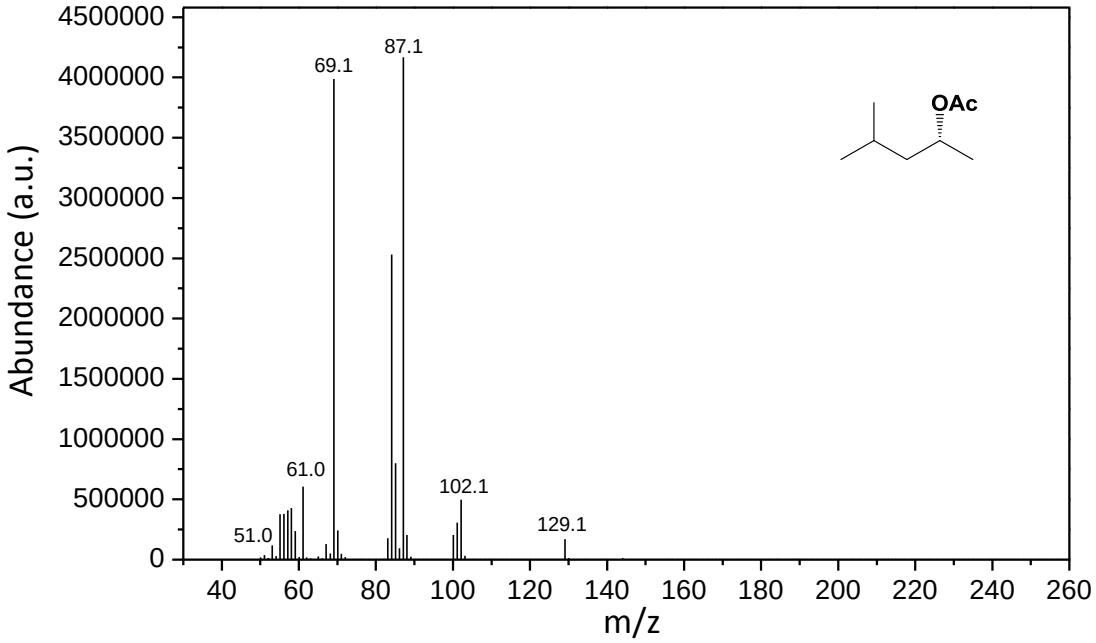
Abundance (a.u.)
m/z
OAc
69.1
87.1
61.0
102.1
51.0
129.1

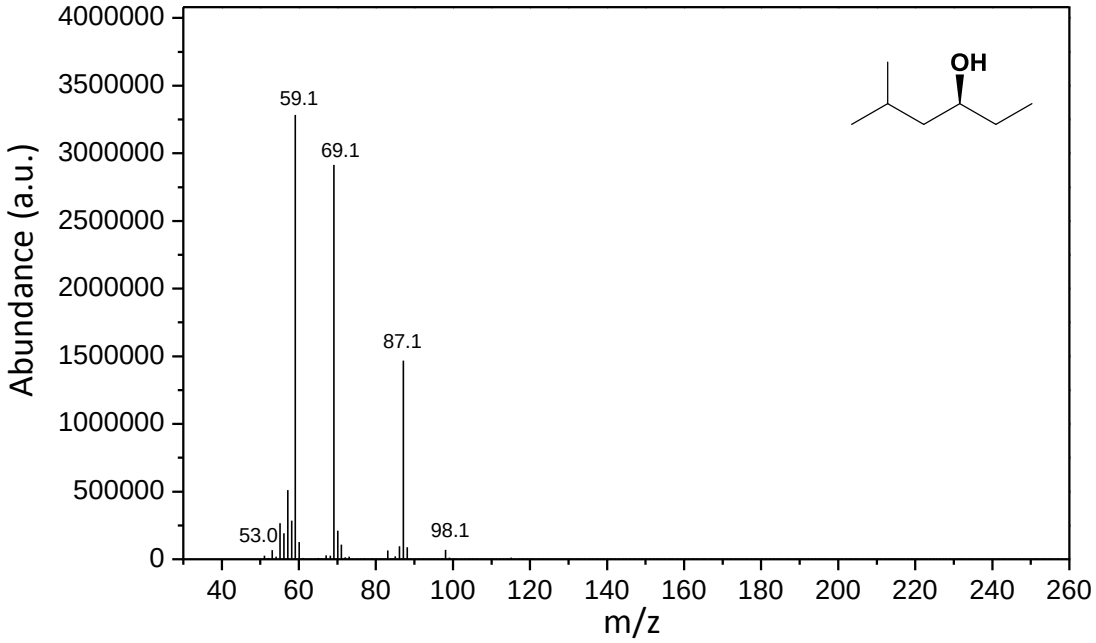
OH
59.1
69.1
87.1
53.0
98.1
Abundance (a.u.)
m/z

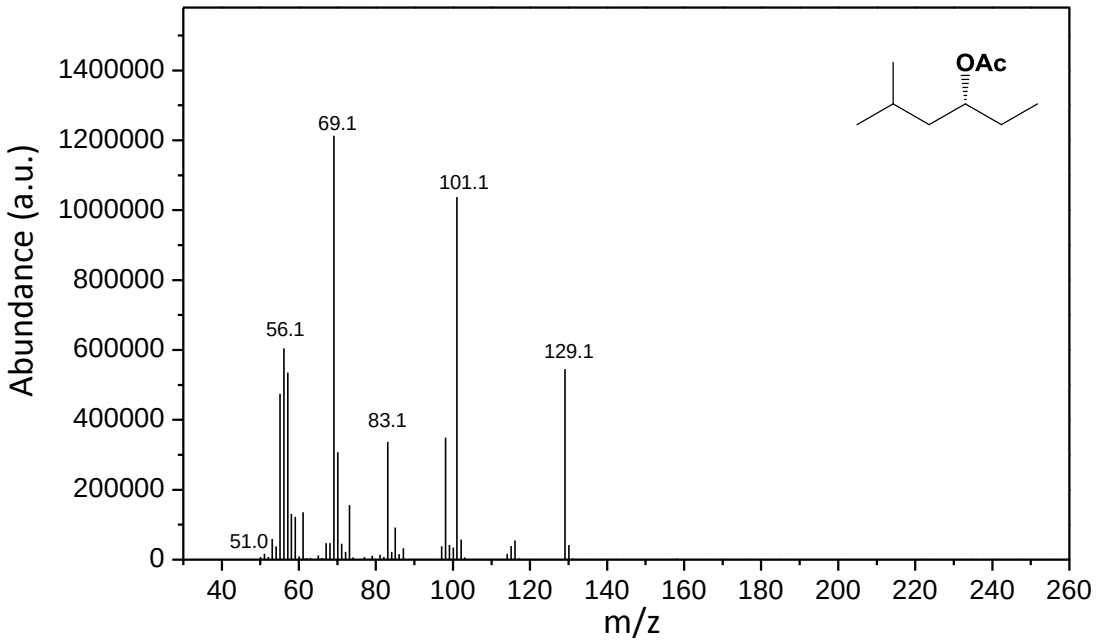
OAc
69.1
101.1
56.1
129.1
83.1
51.0
Abundance (a.u.)
m/z

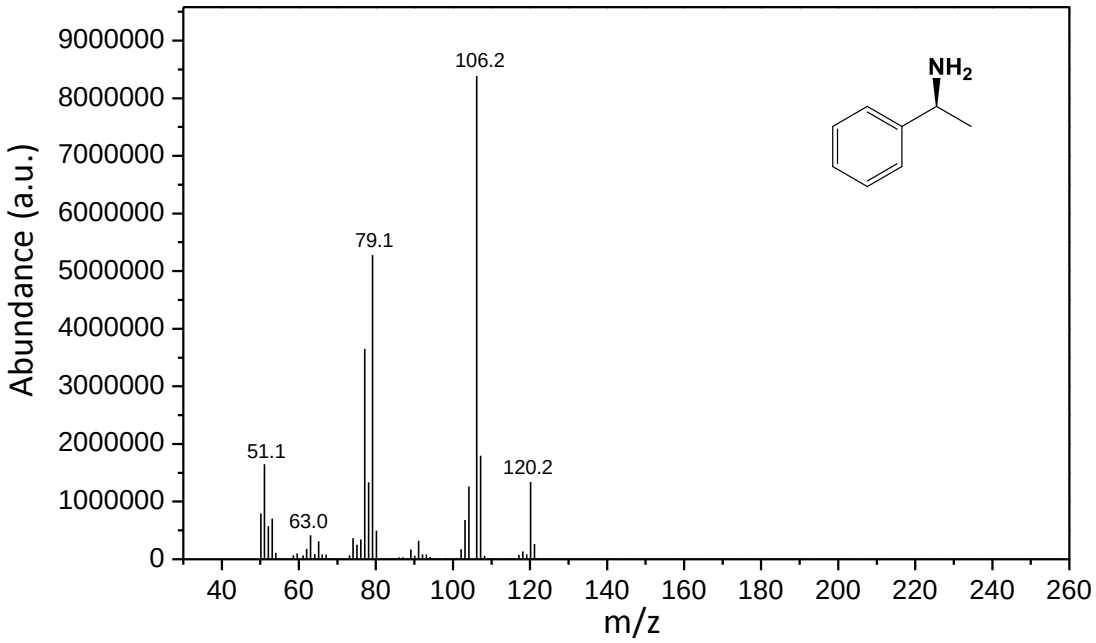
Abundance (a.u.)
m/z
106.2
79.1
51.1
63.0
120.2
NH2

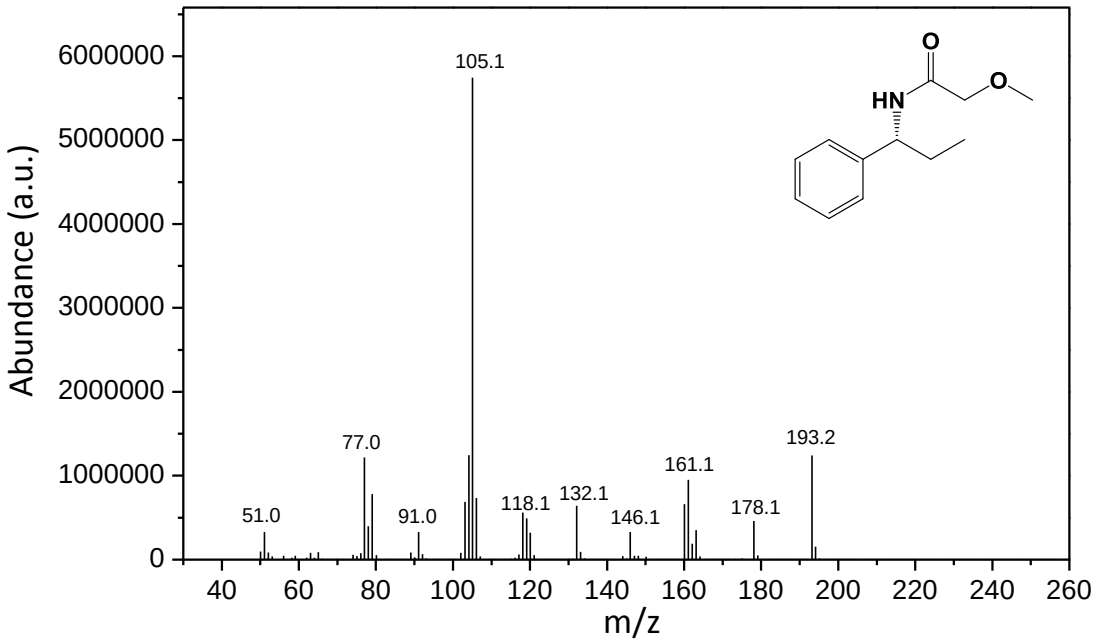
Abundance (a.u.)
m/z
105.1
77.0
51.0
91.0
118.1
132.1
146.1
161.1
178.1
193.2
O
HN
O

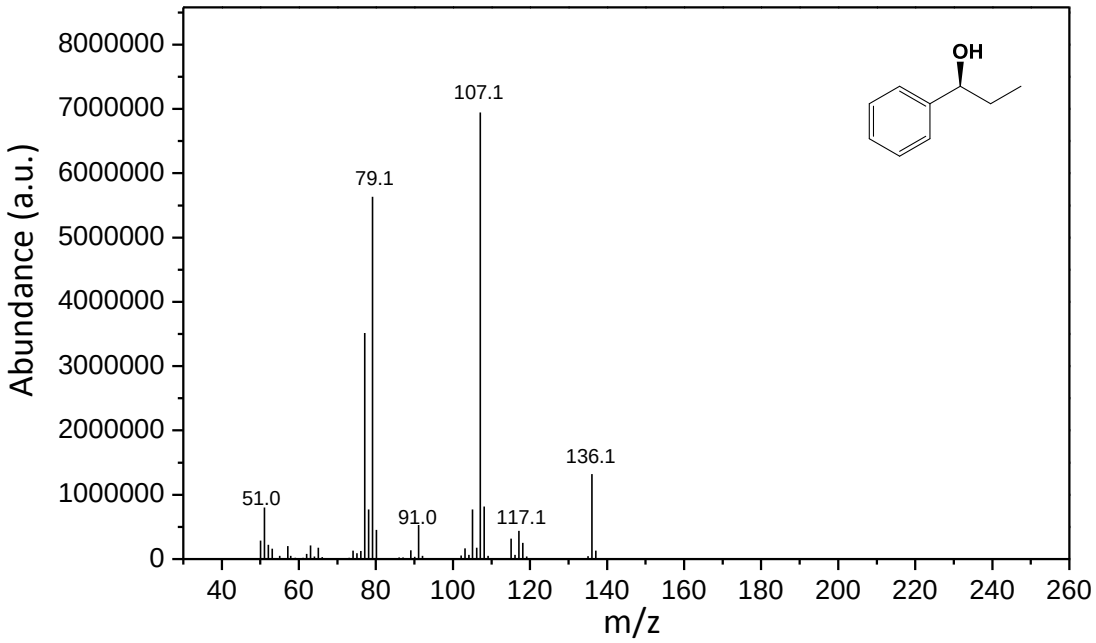
OH
107.1
79.1
136.1
51.0
91.0
117.1
Abundance (a.u.)
m/z

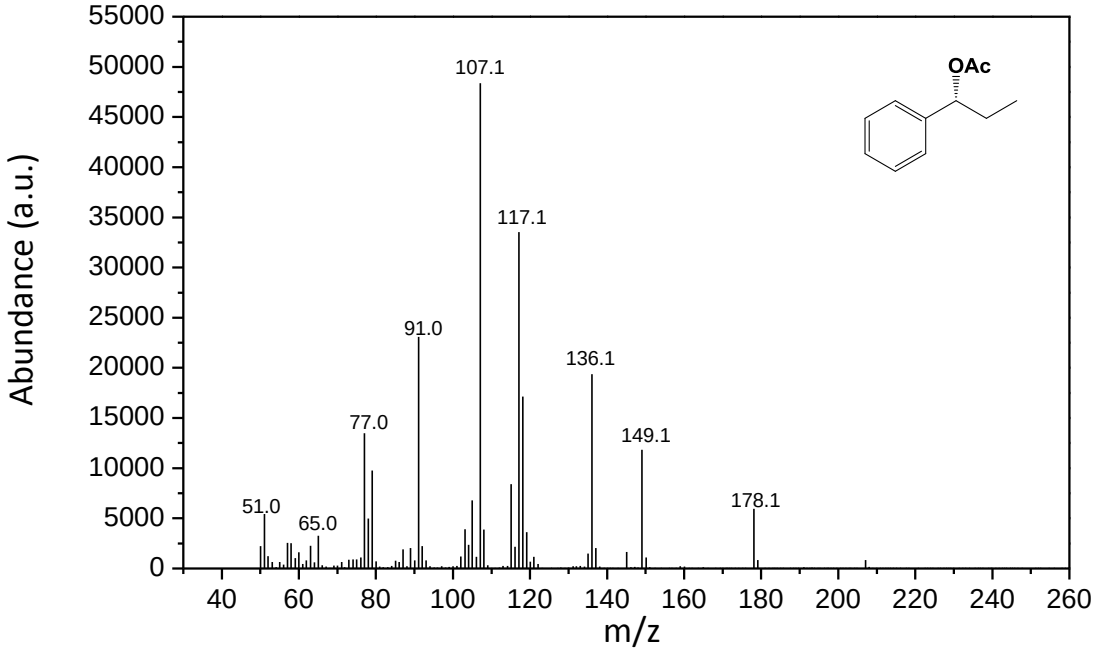
OAc
107.1
117.1
91.0
136.1
77.0
149.1
178.1
51.0
65.0
Abundance (a.u.)
m/z

For CuI-Catalyzed Azide–Alkyne Cycloaddition: